https://doi.org/10.5194/acp-2019-486
Preprint. Discussion started: 26 June 2019


Atmospheric Chemistry and Physics Discussions

# The urban canopy meteorological forcing and its impact on ozone and PM2.5: role of the vertical turbulent transport

Peter Huszar[1], Jan Karlický[1], Jana Ďoubalová[1,2], Kateřina Šindelářová[1], Tereza Nováková[1], Michal Belda[1], Tomáš Halenka[1], Michal Žák[1], and Petr Pišoft[1]

[1]Department of Atmospheric Physics, Faculty of Mathematics and Physics, Charles University, Prague, V Holešovičkách 2, 180 00 Prague 8, Czech Republic
[2]Czech Hydrometeorological Institute (CHMI), Na Šabatce 17, 14306, Prague 4, Czech Republic

**Correspondence:** P. Huszar (huszarpet@gmail.com)

**Abstract.** Urban surfaces due to specific geometry and physical properties bring modified transport of momentum, moisture and heat between them and the air above and perturb the radiative, thermal and mechanical balance resulting in changed meteorological condition (e.g. the UHI - urban heat island phenomenon). From an air quality perspective, many studies argue that one of the most important changes is the increased turbulence enhancing vertical mixing of pollutants above cities, although increased temperatures and wind stilling play an important role too. Using the regional climate model RegCM4 coupled to chemistry transport model CAMx over central Europe we study how urban surfaces affect the vertical turbulent transport of selected pollutants through modifications of the vertical eddy diffusion coefficient ($Kv$). For the period of 2007-2011 and over central Europe numerous model experiments are carried out in order to evaluate the impact of six different methods for $Kv$ calculation on the surface concentrations as well as vertical profiles of ozone and PM2.5 over selected cities (Prague and Berlin). Three cascading domains are set up at 27km, 9km and 3km resolutions, which further enables to analyze the sensitivity to model grid resolution. A number of model experiments are performed where urban surfaces are considered or replaced by rural ones in order to isolate the urban canopy meteorological forcing. Apart from the well pronounced and expected impact on temperature (increases up to 2° C) and wind (decreases up to -2 $\mathrm{ms}^{-1}$) there is strong impact on vertical eddy diffusion in all of the six $Kv$ methods. The $Kv$ enhancement ranges from a few 0.5 up to 30 $\mathrm{m}^2\mathrm{s}^{-1}$ at the surface and from 1 to 100 $\mathrm{m}^2\mathrm{s}^{-1}$ at higher levels depending on the methods, while the turbulent kinetic energy (TKE) based methods produce the largest impact.

The range of impact on the vertical eddy diffusion coefficient propagates to a range of ozone ($O_3$) increase of 0.4 to 4 ppbv near the surface in both summer and winter, while at higher levels, decreases occur from a few -0.4 ppbv to as much as -2 ppbv. In case of PM2.5, enhanced vertical eddy diffusion leads to decrease of near surface concentrations ranging from almost zero to -1 $\mu\mathrm{gm}^{-3}$ in summer and to decreases from -0.5 to -2 $\mu\mathrm{gm}^{-3}$ in winter. Comparing these results to the "total-impact", i.e. to the impact of all considered urban meteorological changes, we can conclude that much of the overall urban meteorological forcing is explained by acting of the enhanced vertical eddy diffusion, which counterweights the opposing effects of other components of this forcing (temperature, humidity and wind impact). The results further show that this conclusion holds regardless of the resolution chosen and in both the warm and cold part of the year. Our study demonstrates the dominant role

https://doi.org/10.5194/acp-2019-486
Preprint. Discussion started: 26 June 2019


Atmospheric Chemistry and Physics Discussions

of turbulent transport of pollutants above urban areas and stresses the need for further investigation how variation of urban land-use influence the pollutant transport from the urban canopy.

## 1 Introduction

Urbanization has numerous effects on the environment while the impact on the atmospheric environment is considered as the most far-reaching (Folberth et al., 2015). This impact acts via multiple pathways. First of all, cities are intense emission hot-spots affecting the air-quality and atmospheric chemistry in general (Im and Kanakidou, 2012; Huszar et al., 2016a) while these modifications occur not only over city scales but propagate to regional and even global scale (Butler et al., 2012; Stock et al., 2013).

Secondly, cities represent distinct surfaces compared to their rural counterparts due to high percentage of artificial coverage with specific geometric layout. These surfaces modify the thermal and radiative balance of the overlaying air resulting in the well-known and documented urban heat island effect (UHI; Oke, 1982; Oke et al., 2017), when urban temperatures are higher than those over rural surroundings depending on the synoptic conditions (Žák et al., 2019). Urban surfaces further represent enhanced drag on winds which results in decrease of average wind speed (Huszar et al., 2014; Jacobson et al., 2015; Zha et al., 2019). On the other hand, this drag trigger mechanical turbulence contributing to the increase of the planetary boundary layer (PBL) height (Roth, 2000; Flagg and Taylor, 2011) and enhanced vertical mixing (Barnes et al., 2014; Huszar et al., 2018b; Ren et al., 2019). It has been also recognized that increased run-off and suppressed evaporation from urban surfaces reduce the humidity (e.g. Richards, 2004) and the so called urban dry island (UDI) effect can form, as recently defined by Hao et al. (2018). Huszar et al. (2014) argued that urbanization contributes to warming of whole regions and largely determines their climate (Květoň and Žák, 2007). Not surprisingly, mitigation strategies of adverse urban climate conditions is an up-to-date research area (e.g. Zhao et al., 2017).

Meteorological conditions are, thus, strongly perturbed over urbanized areas. As air chemistry is closely associated with meteorological variables, the urban induced modifications in meteorological conditions will result in perturbation of species concentrations, as already shown by many authors regarding the meteorological changes due to climate-change and their impact on air pollution (Huszar et al., 2011; Juda-Rezler et al., 2012).

The urban meteorological forcing encompasses many elements and each has a specific impact on air quality, often counter-balancing each other. Higher urban temperatures in connection with UHI modify chemical reaction rates and aerosol nucleation as well as they modify dry deposition and wet scavenging rates (Seinfeld and Pandis, 1998). Although, higher temperatures favor ozone formation (Im et al., 2011), in urban areas the situation can be different. Huszar et al. (2018a) showed that due to higher temperatures alone, surface ozone in urban areas is reduced, while the main contributor to this reduction is the increased dry-deposition velocities and increased flux of nitrogen oxides ($NO_x$) towards nitric acid ($HNO_3$). Sarrat et al. (2006) concluded too that, especially during nighttime, UHI influences the $NO + O_3 \rightarrow NO_2 + O_2$ reaction and ozone dry deposition reducing its concentrations. Tao et al. (2013) calculated increase of dry-deposition due to rural-to-urban transition as well, probably due to higher temperatures. Regarding aerosols, Huszar et al. (2018b) showed that due to elevated urban tempera-

https://doi.org/10.5194/acp-2019-486
Preprint. Discussion started: 26 June 2019


Atmospheric Chemistry and Physics Discussions

tures, gas-to-particle partitioning is limited leading to decrease of the secondary inorganic component of PM2.5 (particles of diameter < 2 μm).

Another component of the urban meteorological forcing is the changed wind pattern and average speed. Wang et al. (2009), Hidalgo et al. (2010), Ryu et al. (2013a) and Ryu et al. (2013b) modeled the UHI-induced urban-breeze circulation resulting in pollutant transport from and to cities. This depends on the daytime but also on the surrounding terrain and coast (Ganbat et al., 2015; Li et al., 2017) and usually leads to increases of urban ozone concentrations. Urban surfaces have however an opposite role too: higher drag due to the urban architecture induces wind stilling which consequently reduces the dispersion of urban emissions and secondary pollutants into larger scales. According to Jacobson et al. (2015), the total column pollution over a megacity is enhanced due to air-stagnation. Due to wind stilling only, Huszar et al. (2018a, b) modeled large increases of primary pollutants ($NO_x$, $SO_2$) and primary components of PM2.5, however $O_3$ is reduced due to increased titration. de la Paz et al. (2016) found that lower wind over urban areas is the main driver of urban surface induced air-quality changes.

Due to surface heterogeneities typical to urban areas, mechanical turbulence is increased and eddy-transport helps pollutant removal from near the surface towards upper layers of urban PBL (Stutz et al., 2004). Indeed, a very strong link is identified between air pollution and the structure of the urban PBL (Masson et al., 2008). It has to be noted here, that emissions occur on street levels that of course cannot be resolved by regional scale models. However, these models can resolve the turbulent layer over the building level where turbulent mixing in the vertical detrains scalars from streets canyons into the turbulent boundary layer above the buildings and the conventional atmospheric turbulence becomes dominant (Belcher et al., 2015). Accordingly, many studies adopted regional scale modeling techniques to describe the urbanization impact on species concentrations. Martilli et al. (2003) and Sarrat et al. (2006) focused on Paris and Athens and found significant pollutant decrease, mainly due to enhanced turbulence when urban surfaces are considered. Reduction of primary pollutants ($NO_x$ and CO) due to enhanced vertical mixing due to urbanization is modeled by Struzewska and Kaminski (2012) too. If mitigation measures are implemented to reduce UHI, the consequent reduction of PBL height and vertical turbulent transport causes increase of primary pollutants but decrease of ozone over the surface (Fallmann et al., 2016). Large Chinese agglomerations of Pearl River Delta and Yangtze River Delta (PRD and YRD) have been subject of numerous studies and all argued that urbanization induced increase of vertical turbulent transport favors the reduction of primary pollutants (e.g. $NO_x$) but this leads to enhancement of e.g. ozone (Wang et al., 2007, 2009). Zhu et al. (2015) arrives to similar conclusions but finds larger ozone changes over higher model levels. Xie et al. (2016a) and Xie et al. (2016b) argued that the urban induced enhancement of vertical eddy-transport is important especially during summer and arrives to expected conclusions, i.e. decrease of primary and increase of secondary pollutants (ozone). Both Zhong et al. (2017) and Zhong et al. (2018) predict stronger vertical transport too and emphasize its major role, but they also look at the simultaneous effect of urban emissions and their radiative effects and conclude that the decrease of surface concentrations is out-weighed partly by the PBL stabilization due to aerosol radiative cooling. Enhanced vertical eddy-transport due to the introduction of urban surfaces is the main driver of PM10 (particle matter of diameter < $10\mu m$) as found by Zhu et al. (2017). Liao et al. (2014) applied a range of urban canopy models (UCM) within a mesoscale model and found that those UCMs that produce deeper PBL predict stronger reduction of PM10, underlining the dominant role of urban turbulence. Urban enhanced vertical eddy-diffusion was found to be the primary factor that led to $SO_2$ decreases over

https://doi.org/10.5194/acp-2019-486
Preprint. Discussion started: 26 June 2019


Atmospheric Chemistry and Physics Discussions

Chinese cities in Chen et al. (2014). Kim et al. (2015) showed for Paris (France) that using urban canopy models that support stronger vertical mixing in the model over urban areas, $PM_{2.5}$ concentrations become lower and fit better to observations. In Ren et al. (2019), the turbulent effects caused by urban expansion reduces the urban canopy pollution under otherwise same weather and emission intensities. Li et al. (2019a) recently analyzed the benefits to use a detailed large-eddy simulation (LES) of urban boundary layer compared to mesoscale model representation of turbulence and found that vertical turbulence is a dominant process that determines the pollutant's removal from urban areas, however LES provides more homogeneous ozone and $NO_x$ profiles that have a better agreement with observational data, as they argued. Li et al. (2019b) using the WRF model analyzed the urbanization induced air-quality changes over California (U.S.) and found that the main driver of ozone and PM2.5 changes are the changes in ventilation, i.e. both wind speed and vertical eddy diffusion seems to play a very important role. Janssen et al. (2017) analyzed the modifications of primary and secondary organic aerosol (POA/SOA) and found that the PBL increase and enhanced turbulence over cities have opposing effects on these two aerosol components: while POA decreases due to increased removal, increase are encountered for SOA due to stronger downward transport from the residual layer (RL). Finally, the role of the intermittent turbulence in removing PM2.5 from near the surface over urbanized areas was recently examined by Wei et al. (2018).

As seen above, the vast majority of the authors argue that the turbulence is a dominant if not the most important factor that determines the overall impact of urban induced meteorological forcing on air-quality. On the other hand, a very few of them looked at the individual impact of each perturbed meteorological parameters (temperature, wind, turbulence). Recently, in our previous works, Huszar et al. (2018a, b), we modeled the impact of urbanization on meteorological conditions and, consequently, on air-quality using a regional scale, offline coupled climate-chemistry model system. Besides the total impact, we looked at the isolated impact of changed temperature, humidity, wind and vertical eddy diffusion coefficient ($Kv$) and our results underlined the findings of previous authors. The impact of changed $Kv$ values indeed dominates the overall impact however different part of the day other impacts can counterbalance and become dominant. We found that during night time, the temperature impacts PM2.5 concentrations more (resulting in increase) than the increased turbulence (resulting in decrease). Furthermore, it turned out clear that the total impact of the combined effect of different meteorological parameters is, in fact, a result of counteracting effects of opposite signs but comparable magnitudes. In vast majority of papers listed above, and confirmed by our previous findings, the impact of enhanced vertical eddy-diffusion turned out to be the strongest one. The vertical eddy diffusion coefficient that enters the chemistry transport models coupled online or offline to the driving mesoscale models are usually parameterized or diagnosed from large scale fields as wind, temperature, PBL height or the prognostic turbulent kinetic energy (depending on the PBL scheme used). Question arises here, how the uncertainty that comes from calculating $Kv$ values propagates to the urban impact on species concentration and whether the dominant role of the turbulence impact will hold if using other options for $Kv$ calculation.

Our paper is motivated by the question above and its primary objective is to evaluate, how the regional scale model representation of vertical diffusion ($Kv$) of scalar variable (e.g. pollutant concentration) affects the impact of urban areas on air-quality via the urban meteorological forcing. In other words, we are interested how a range of methods for $Kv$ calculations translates to a range of $Kv$ values, how this propagates to the impact of urbanization on vertical diffusion and finally, what range of

https://doi.org/10.5194/acp-2019-486
Preprint. Discussion started: 26 June 2019


Atmospheric Chemistry and Physics Discussions

impact on species concentrations this will consequently lead to. Our focus will be ozone and PM2.5 concentrations. Further, the study aims to answer if the dominance of the $Kv$-impact holds if using $Kv$ calculation methods alternative to the default one (CMAQ; used e.g. in Huszar et al., 2018b). This work is a follow-up study to our previous works, Huszar et al. (2018a) and Huszar et al. (2018b), and extends them by focusing on the vertical eddy-diffusion which appears to be a major factor in the urban-air quality coupling. Moreover, the effect of horizontal resolution, a key factor in regional chemistry-climate modeling, is evaluated here too and our focus is extended to winter months (DJF) as well. A tailored chain of model experiments is implemented to achieve this goal detailed in the next section. The results are then presented in Section 3 which encompasses the model validation, the impact on meteorological parameters as well as the impact on air-quality. Finally, the results are discussed and conclusions are drawn.

## 2 Experimental setup

### 2.1 Models

#### 2.1.1 RegCM4

The regional climate simulations were performed by the model RegCM (version 4.6) (Giorgi et al., 2012) servings as a meteorological driver for the chemistry transport model simulations (see further). RegCM4 is a non-hydrostatic mesoscale climate model developed at Internation Centre for Theoretical Physics (ICTP) based on the MM4 model. It offers multiple methods for calculating convection; here the Tiedtke scheme was chosen (Tiedtke et al., 1989). Cloud and rain microphysics is computed using the explicit moisture scheme of Nogherotto et al. (2016) which offers a more comprehensive treatment of moisture and its transformations in air compared to the older SUBBEX scheme (Pal et al., 2000). For radiative transfer, the NCAR Community Climate Model Version 3 (CCM3; Kiehl et al., 1996) was used.

The planetary boundary layer processes were treated using the UW (University of Washington) method developed by Grenier and Bretheron (2001) and Bretherton et al. (2004). This scheme provides an alternative to the default non-local diagnostic Holtslag PBL scheme (HOL; Holtslag et al., 1990) originally included in RegCM. The UW is a local prognostic 1.5-order scheme. Giorgi et al. (2012) made tests to identify the differences between these PBL parameterizations and they found excessive vertical turbulent transfer in the HOL scheme for heat and water vapor leading to large biases in winter temperatures and problems capturing low level stratus. The UW scheme seemed to overcome this shortcoming. Another reason for choosing this scheme in our simulations was that it provides prognostic turbulent kinetic energy (TKE) values on model output which enables to use TKE-based estimation of vertical eddy-diffusion coefficient. Moreover, UW itself contains such a method (see further) and directly supplies $Kv$ values upon model output readily usable in chemistry-transport model calculations.

Landcover processes are calculated with the Community Land Model version 4.5 (CLM4.5; Lawrence et al., 2011; Oleson et al., 2013). CLM4.5 contains the CLMU urban canopy module (Oleson et al., 2008a) which considers the classical canyon representation of urban geometry. The canyon is bounded by roofs, walls and canyon floor, and trapping of solar and long-wave radiation within is considered.

https://doi.org/10.5194/acp-2019-486
Preprint. Discussion started: 26 June 2019


Atmospheric Chemistry and Physics Discussions

Within the urban canyon, momentum fluxes are calculated using a roughness lengths and displacement height typical for the canyon environment. Anthropogenic heat flux from air conditioning and heating is computed within the urban canopy model from the heat conduction equation based on an interior boundary conditions corresponding to interior temperature of the building. To this heat flux, waste heat from air heating/conditioning is further added. It is parameterized directly from the amount of energy required to keep the internal building temperature between a prescribed maximum and minimum values, assuming 50% efficiency of the heating/cooling systems (Oleson et al., 2008b).

### 2.1.2 CAMxv6

The chemical simulations were performed with the chemistry transport model (CTM) CAMx version 6.50 ENVIRON (2018). CAMx is an Eulerian photochemical CTM that implements multiple gas phase chemistry schemes (CB5, CB6, SAPRC07TC). The CB5 scheme (Yarwood et al., 2005) was invoked in this study having optimal complexity for long term climate scale simulations. Particles sizes are considered using static two mode approach. Dry deposition is solved using the Zhang et al. (2003) approach while for wet deposition the Seinfeld and Pandis (1998) method is applied. The ISORROPIA thermodynamic equilibrium model (Nenes and Pandis, 1998) is also activated in our set-up to calculate the composition and phase state of the ammonia-sulfate-nitrate-chloride-sodium-water inorganic aerosol system in equilibrium with gas phase precursors. Secondary organic aerosol (SOA) is computed with the semi-volatile equilibrium scheme SOAP (Strader et al., 1999).

CAMx is offline coupled to RegCM using the meteorological preprocessor RegCM2CAMx originally developed by Huszar et al. (2012). For the diagnostic calculations of the vertical eddy diffusion coefficients ($Kv$), originally, the OB70 (O'Brien, 1970) method was implemented in RegCM2CAMx that uses a simple prescription of the $Kv$ profile. Huszar et al. (2016a) extended RegCM2CAMx by the CMAQ scheme (Byun, 1999) implemented in CMAQ which applies the similarity theory for different stability regimes of the boundary layer. The stability regime in CMAQ method is defined using the dimensionless ratio of the height above the ground and the Monin-Obukhov length. Here, we further extended the range of possible turbulent diffusion packages with a nonlocal turbulent mixing scheme YSU (Hong et al., 2006) which contains an explicit treatment of entrainment processes at the PBL top. We also added the ACM2 method (Pleim, 2007) which is a new version of the original asymmetric convective model (ACM) and includes the nonlocal scheme of ACM combined with an eddy diffusion scheme. ACM2 is thus capable to represent both the supergrid and subgrid components of turbulent transport. The fifth $Kv$ calculation method (MYJ – Mellow-Yamada-Jancic) is based on the TKE approach of Mellor and Yamada (1982) as implemented by Janjic (1994). MYJ implements 1.5-order (level 2.5) turbulence closure mode and determines the eddy diffusion coefficients from prognostic TKE. Finally, the last method of calculating $Kv$ for CAMx is to read them directly from RegCM output (denoted as the DIRECT method). In fact DIRECT and MYJ differ only in the implementation but are based on the same physical principles. In summary, a range of six $Kv$ calculation methods (CMAQ, DIRECT, ACM2, OB70, MYJ and YSU) are available to translate RegCM outputs to CAMx ready $Kv$ fields representing a wide range of values to drive vertical eddy diffusion (see further). It is clear that by this approach the calculation of $Kv$ values are based sometimes on different concept than the calculation of PBL characteristics in the driving meteorological model (e.g, TKE based PBL scheme in RegCM and similarity theory in CMAQ $Kv$-scheme). However, all $Kv$ methods use only large scale characteristic from the meteorological

https://doi.org/10.5194/acp-2019-486
Preprint. Discussion started: 26 June 2019


Atmospheric Chemistry and Physics Discussions

model as input (like wind, temperature, humidity, TKE profile, PBL height etc.) without any a priory expectation on how these physical quantities have been obtained. In this regard we assume this "non-consistency" a minor issue. Furthermore, Lee et al. (2011) showed too that using "non-consistent" method in calculating $Kv$ for CTMs does not implicate less accurate results than directly coupling the PBL parameters.

It has to be noted, that the dry deposition scheme used in CAMx does not depend directly on the $Kv$ values provided on CAMx inputs. Instead, for the aerodynamic resistance used for calculation of diffusion trough the first model layer to the ground is computed using the scheme of Louis (1979) based on the on solar insolation, wind speed, surface roughness, and nearsurface temperature lapse rate. Consequently, different $Kv$ computation methods does not directly impact dry deposition velocities.

Further developments of RegCM2CAMx here include that it takes cloud/rain/snow water directly from RegCM output, which in the version used already enables to output these variables. No feedbacks of the modeled species concentrations on RegCM radiation/microphysical processes were considered. Huszar et al. (2016b), using a similar setup than here showed that urbanization induced chemical changes have a very small radiative feedback in long-term average.

### 2.2 Experimental setup and data

Model experiments were performed over three telescoping domains of the following horizontal resolution(size – as gridboxes): 27 km(189 x 141), 9km(189 x 165) and 3 km(93 x 69). Each domain is centered over Prague, Czech republic (50.075° N, 14.44° E) and uses the same projection parameters (Lambert Conic Conformal). Accordingly, the three domain is denoted PHA27, PHA09 and PHA03. The regional climate model simulations were performed over 23 vertical levels for the 27 km domain. For the higher resolution ones, this is increased to 41 levels. The lowermost level is about 60-70 m thick while the model top is at 50 hPa. Within the RegCM runs, the outer 27 km domain was forced by the ERA-interim reanalysis (Simmons et al., 2010). The nested 9 and 3 km domains are forced by the corresponding parent domain using one-way nesting. The 27 km simulations were calculated in hydrostatic mode while the rest, due to higher resolution, required non-hydrostatic approach.

The chemistry-transport model experiments were performed over same domains and use 18 vertical layers. These are identical to the first 18 layers of the PHA27 domain. For the 9 and 3 km runs, the lowermost CAMx layers are identical to RegCM layers too, for higher ones, layer collapsing was applied. The chemical simulation for the 27 km domain were forced by the MOZART-4 global CTM runs forced by NCEP reanalysis (Emmons et al., 2010). The inner domains were one-way nested similarly to the regional climate model runs.

Landuse information was derived from the CORINE CLC 2012 landcover data (https://land.copernicus.eu/pan-european/corine-land-cover) and the USGS database where CORINE was not available. The urban geometry parameters are taken from the $0.05° \times 0.05°$ resolution LandScan dataset which provides average building heights (H), urban canyon height-to-width ratios (H:W), and fraction of pervious surface (e.g., vegetation), roof area, and impervious surfaces (e.g., roads and sidewalks) are provided. Within CLM4.5, urban landuse type is represented as a fraction in percentages of urban intensity categories (HD, MD, LD and TBD). This gives a reasonable description of urban coverage at all resolutions (even at low resolution, small cities are accounted for as low percentage value).

https://doi.org/10.5194/acp-2019-486
Preprint. Discussion started: 26 June 2019


Atmospheric Chemistry and Physics Discussions

The TNO MACC-III (an update of the previous version II Kuenen et al., 2014, ;) data were used as emissions for Europe except Czech republic, where a high resolution national Register of Emissions and Air Pollution Sources (REZZO) dataset issued by the Czech Hydrometeorological Institute (www.chmi.cz) and the ATEM Traffic Emissions dataset provided by ATEM (Studio of ecological models; www.atem.cz) was used. The listed emissions sources contain annual emissions of the main pollutants, namely $NO_2$, $SO_2$, $NO_x$, CO, volatile organic compounds VOC, PM2.5 and PM10. MACC-III data are gridded data, while the Czech REZZO and ATEM datasets are defined as area, point and line (for road transportation) shapefiles of irregular shapes corresponding to counties, major sources and roads.

The raw emission data is preprocessed using the Flexible Universal Processor for Modeling Emissions (FUME) emission model (Benešová et al., 2018, ; http://fume-ep.org/). FUME is intended primarily for the preparation of CTM ready emissions files. As such, FUME is responsible for preprocessing the raw input files and the spatial distribution, chemical speciation, and time disaggregation of input emissions. Emission are provided in 11 activity sectors (SNAP – Selected Nomenclature for sources of Air Pollution) and sector specific time-dissaggregation (van der Gon et al., 2011) and speciation factors (Passant, 2002) are applied to spatially interpolated emissions to derive hourly speciated emissions for CAMx. Biogenic emissions of hydrocarbons (BVOC) are calculated using the MEGANv2.1 emissions model (Guenther et al., 2012).

Being an offline couple, first the RegCM model experiments were carried out. After, the meteorology-dependent BVOC emissions were computed by MEGAN while for each gridbox, the fractional cover of different plant functional types and their emission factors determine the actual BVOC emission flux (i.e. for urban gridboxes it can be even zero). In next, the meteorological inputs for CAMx are generated. Finally, BVOC emissions are combined with the anthropogenic emissions calculated by FUME. Having or inputs prepared, a series of CAMx simulations for the 2007-2011 period were conducted for each model domain and these are summarized in Tab. 1. For RegCM, a pair of model experiments were performed denoted "URBAN" and "NOURBAN" where urban landsurface was considered (and modeled with the CLMU model within RegCM) or replaced by rural surface most typical for the surroundings of the particular city. This meant crops in most of the times. The urban effect were calculated thus using the "annihilation method" (Baklanov et al., 2016), which has been often employed for urban studies but also for transport related impact assessment (Huszar et al., 2013, e.g.).

Using RegCM meteorology, numerous of CAMx runs were carried out depending on which urban meteorological effects are considered and which $Kv$ calculation method is employed. The "NOURBAN" reference CAMx run is driven by RegCM meteorology that does not consider any urban meteorological forcing: i.e. no temperature, humidity, wind and turbulence effects, which means it is driven by the NOURBAN RegCM runs. These CAMx experiments implement the CMAQ method for $Kv$ calculation which is the default option and was used also in Huszar et al. (2018a, b). Within the impact of the simulated meteorological changes on chemistry, the following effects were taken into account 1) modified temperature (t-impact); 2) modified absolute humidity (q-impact); 3) modified wind speed (uv-impact) and 4) modified vertical eddy diffusion coefficient; kv-impact). In a further set of simulations, denoted "URB_t+q+uv+kv", all the listed effects were considered and finally, in the "URB_t+q+uv" simulations, the kv–impact was removed. In addition, the "URB_t+q+uv+kv" and the "URB_t+q+uv" simulations were repeated with all listed $Kv$ calculation methods. In this way, the total urban impact can be evaluated as the difference between the corresponding URB_t+q+uv+kv and NOURBAN model experiments. However, the main focus

https://doi.org/10.5194/acp-2019-486
Preprint. Discussion started: 26 June 2019


Atmospheric Chemistry and Physics Discussions

of the paper is the kv-impact (as URB_t+q+uv+kv minus URB_t+q+uv), which is now possible to evaluate by six different representations of vertical eddy diffusion. Each listed simulation is repeated for all model domain which allows to assess the sensitivity of results on horizontal model resolution too. In case of the representation of meteorological conditions in AQ modeling, this can be relatively large (Tie et al., 2010). Finally, it has to be noted that for chemical simulations, the landuse was kept the same for all model experiments in order to isolate the effect of meteorological changes on air quality.

## 3 Results

### 3.1 Model validation

#### 3.1.1 Model climate

The simulated model results were validated against observational data. For meteorology, the gridded E-OBS van der Besselaar et al. (2011) data were chosen which enables spatial comparison. The modeled average summer (JJA) and winter (DJF) surface temperatures and precipitation are evaluated for all model resolution. Note that from the 27 km model domain result are shown only over a subdomain corresponding to the 9 km domain for easier comparison. In Fig. 1, the difference between the model near surface temperature and observation is presented. During summer, the 27 and 9 km resolution runs tend to underestimate surface temperatures by 2° C, while the 9 km run have smaller biases and even some overestimation occurs over the eastern part of the domain up to 1° C. Largest differences are encountered over mountainous areas where the main reason lies probably in the poor model representation of complex orography. The 3 km run shows a warm bias almost everywhere (except a few areas near the Czech border) up to 1-2° C. For the winter months, all three resolutions shows a warm model bias, which is lowest in the 27 km run (up to 2° C) and reaches 3° C in the 3 km model experiment. Notably, the warm bias is largest over Prague (indicated by its borders) which suggest that the model overestimates the urban temperature effects.

The difference between the model total precipitation and observation is shown in Fig. 2 in $\mathrm{mmday}^{-1}$. During winter, precipitation is overestimated in RegCM at each resolution reaching up to 3-4 $\mathrm{mmday}^{-1}$ above mountains. The medium resolution model experiment shows somewhat smaller bias while at 3 km around Prague, the model overestimated rain by 2-3 $\mathrm{mmday}^{-1}$. A different picture is seen during JJA: the low resolution run show a strong overestimation of the precipitation by up to 2-3 $\mathrm{mmday}^{-1}$ all over the domain. A much smaller positive model bias is encountered for the 9 km with values usually lower than 1 $\mathrm{mmday}^{-1}$ (with even some negative bias over the domain edges). Regarding the 3 km domain, both positive and negative biases are present in the range of -3 to 2 $\mathrm{mmday}^{-1}$. For the area of Prague, the bias is however small, lying between -0.5 to 0.5 $\mathrm{mmday}^{-1}$.

#### 3.1.2 Air quality

The modeled surface concentrations were confronted with the European Environment Agency Airbase (https://www.eea.europa.eu/data-and-maps/data/aqereporting-8) observational data. Rural and urban background stations were selected which

https://doi.org/10.5194/acp-2019-486
Preprint. Discussion started: 26 June 2019


Atmospheric Chemistry and Physics Discussions

are not affected by local sources unresolved by the models (i.e. traffic stations were not considered). The validation focuses on the two key pollutants, $O_3$ and PM2.5.

In Fig. 3 the scatter plots of the comparison of measured and modeled ozone values are shown. It is seen that vast majority of the values lies within a factor of 2 except in winter season when observations exhibit very low values that are not resolved by the model, regardless of the relatively high resolution (3km). In summer, model values are usually overestimated and the overestimation is slightly higher in 27 and 9 km domain. It is also evident that the model provides a narrower range of values than the measurements, especially during summer months when it is unable to capture low ozone situations (large number of observation near zero, while model values are around 50 to 150 $\mu gm^{-3}$).

The deviations seen in the scatter plots are better understood looking and the comparison of average seasonal diurnal cycles. This is shown in Fig. 4. For summer months, the average daily maximum ozone is reasonably captured with a little positive bias around 3-5 $\mu gm^{-3}$ over the 27 and 9 km domains while urban stations have this bias slightly larger. The daily maximum ozone values are almost perfectly captured for the 3 km resolution with a small overestimation for the urban stations. The timing the of maximum is reasonably captured too. However, the model tends to strongly overestimate nighttime values of ozone for all resolution and especially for urban stations. This explains the overall overestimation of average daily ozone values seen in the scatter plot. For winter months, model biases are smaller. For rural stations, model underestimates measured values for the 27 km run and slightly overestimates for the higher resolution domains. Here, however, the daily maximum ozone is well modeled. The observed urban values are overestimated by the model, especially during morning hours by up to 10 $\mu gm^{-3}$, however, again, maximum daily values are reasonably captured. The comparison of monthly means in Fig. 5 confirms the overestimation of ozone values during JJA (by 10-20 $\mu gm^{-3}$), where the main contributor are the too high ozone values during night as seen from previous figure. On the other hand, winter (and spring) averages are modeled with higher accuracy and even some underestimation by model occurs for the 27 km domain (seen also in the diurnal cycles). Again, the positive model bias is somewhat larger for urban stations than background ones.

The daily PM2.5 scatter plots in Fig. 6 and the corresponding normalized mean bias (NMB) values suggest that PM2.5 is underestimated in the model, except for summer over rural stations in the 27 km model experiment. On the other hand, a very good agreement in terms of this metrics is achieved for the 3 km run during JJA. It is seen that the underestimation is caused mostly by the high-end of the observed values which CAMx is not able to resolve. The ratio of modeled value within the ratio of 2 (FAC2) is about 0.6-0.7 at each resolution and season and surprisingly it is usually higher for urban stations. The gain in using higher resolution is not clear and the model improvement depends which metrics is analyzed. For rural stations however, the 3 km model experiments seem to be more accurate than the lower ones.

The monthly values in Fig. 7 brings some light to the root of model biases seen in scatter plots. Winter concentrations are underestimated by the model in each case by about 5-10 $\mu gm^{-3}$ over rural stations and 10-15 $\mu gm^{-3}$ over urban ones. During JJA and for rural stations, model concentrations of PM2.5 tend to be higher then the measured ones by about 3-4 $\mu gm^{-3}$ for the 27 km run, somewhat smaller for the 9 km run (about 2 $\mu gm^{-3}$) and are in a very good agreement for the fine resolution model experiment. Over urban stations, model is consistently lower in PM2.5 concentrations – here, however, the highest underestimation for JJA occurs for the 3 km model experiment (around 3-5 $\mu gm^{-3}$).

https://doi.org/10.5194/acp-2019-486
Preprint. Discussion started: 26 June 2019


Atmospheric Chemistry and Physics Discussions

It has to be noted, that many urban background stations selected in the analysis are taken from small urban areas that are not resolved by model well. Therefore the urban model concentrations are only slightly different from rural ones (higher values for PM2.5 in urban areas and lower ones for $O_3$ due to titration effects).

### 3.2 Impact on meteorology

In our recent papers, Huszar et al. (2018a, b), we showed that urban surfaces largely influence summer values of temperature, humidity, wind speed and the vertical eddy diffusion coefficient (determines the vertical turbulent transport). Here, we extend our analysis to winter months too as well as to the sensitivity on the chosen model resolution. It is widely known, that during winter months, buoyant turbulence is suppressed and the mechanical one governs. Our analysis extended for DJF thus brings new insight on how the urban canopy meteorological forcing acts on air-quality under substantially different weather conditions compared to summer. Another important parameter to meso-scale modeling of urban meteorological effects is the model resolution which determines how well the urban landuse heterogeneity is represented as well as the (meso-)synoptic weather features that strongly influence the urban canopy meteorological effects (e.g. UHI; Žák et al., 2019). The urbanization induced meteorological effects will be evaluated as the difference between RegCM experiments URBAN and NOURBAN (applying the annihilation method). In spatial figures, we will show results for central European region that covers two large cities we focus on, Berlin and Prague. These two cities will be in focus in the diurnal cycle figures too (expect for results on the 3 km domain which cover only Prague).

#### 3.2.1 Temperature

In Fig. 8 the spatial impact of urban surfaces on near surface temperature is shown. In general, DJF impact on temperature is, in average, higher for both cities and exceeds 2 °C. In summer, the impact lies between 1.5 and 2 °C. Over Berlin, the 9 km simulation results in more pronounced impact in both seasons. Over Prague, the impact is highest for the 27 km simulation in both seasons. It is also seen that if spatially averaged over coarse resolution, the 3 km impact over Prague will be lower than over the 9 km and, especially, over the 27 km simulation. Further the figure shows that most of the area analyzed exhibits statistically significant temperature impact suggesting that even minor urbanized areas (small cities, villages) play role in modulating temperature.

The diurnal cycle of the absolute urban temperatures and the urban impact is show in Fig. 9. It is seen, that higher resolutions exhibit warmer urban temperatures in correspondence with the conclusions made in the validation. According to the expectation, maximum urban warming occurs during evening around 8-10 pm UTC (10-12 pm local time) for JJA. For DJF, the maximum difference occurs at different times over each city: for Berlin, it is around midnight UTC (1 am local time) however, over Prague it occurs earlier around 4-8 pm UTC (5-9 pm local time). Over Berlin, the 9 km simulation results in almost 2 times higher impact (1 ° C vs. 2 ° C). Over Prague, the situation differs: the highest impact, in contrary to the absolute values, occurs for the 27 km simulation for winter, however, for summer the three resolutions are very close to each other and show maximum warming around 2.4 ° C.

https://doi.org/10.5194/acp-2019-486
Preprint. Discussion started: 26 June 2019


Atmospheric Chemistry and Physics Discussions

#### 3.2.2 Wind speed

In Fig.10 the summer and winter average impact on 10 m wind speed is shown for the three resolutions. It is seen that the wind is significantly decreased over urban areas while the decrease is higher in DJF (around -1.5 to -2 $\mathrm{ms}^{-1}$) than during JJA (-1 $\mathrm{ms}^{-1}$). The smalled decrease is modeled for the 27 km simulation for both cities and seasons. Statistically significant changes on the 98% level are modeled over large part of the analyzed regions suggesting that even small urban areas contribute to the wind stilling significantly.

Regarding the diurnal cycle of the wind-impact, Fig. 11, it is seen in terms of absolute values, that the two analyzed cities behave somewhat differently: while over Berlin, the 27 km resolution run produce lower winds than the 9 km ones, over Prague the lowest wind speeds are modeled for the highest resolution (and the opposite for the 27 km run). A more unique picture, in accordance with the spatial figures) is seen for the impact itself. The higher the model resolution the stronger is the impact on winds. For Berlin, it reaches -1.5 $\mathrm{ms}^{-1}$ for both seasons during noon. For Prague, the wind impact reaches -1.4 $\mathrm{ms}^{-1}$ for summer and can be as strong as -1.8 $\mathrm{ms}^{-1}$ during winter.

#### 3.2.3 Vertical eddy diffusivities

The main focus of this paper is the urban impact on the vertical eddy diffusion coefficient as a key factor determining urban pollution transport. Here we present this impact for each of the $Kv$-methods that are listed in Section. 2.1.2. In Fig. 12 the urbanization induced changes of the JJA eddy diffusion coefficient at the first model level (approximately 65m, i.e. above the urban canopy layer) are shown for all three model resolutions (rows) and six $Kv$-methods (columns). It is clear from each methods/resolution that $Kv$ values are affected the most over the two selected large cities (Berlin and Prague), however statistically significant changes occur over rural areas too. The most striking feature is the wide range of $Kv$ changes (increases). The smallest urban increase is in generally obtained for the CMAQ and YSU schemes: in both cases the rural-to-urban transition results in about 1-2 $\mathrm{m}^2\mathrm{s}^{-1}$ increase of $Kv$ over both Prague and Berlin. The strongest increase is achieved with the TKE based DIRECT and MYJ methods where it reaches 15 $\mathrm{m}^2\mathrm{s}^{-1}$ for DIRECT and 30 $\mathrm{m}^2\mathrm{s}^{-1}$ for the MYJ methods. The ACM2 and OB70 method lie in the middle range with increases up to 6-10 $\mathrm{m}^2\mathrm{s}^{-1}$. Regarding the sensitivity of the resolution, the effect seems to be small and the three gridsizes result in comparable change of $Kv$ values while often the 27 km resolution produces the strongest impact, especially when spatially averaging of the higher resolution results to 27 km. In summary, the urbanization induced $Kv$ changes above the urban canopy layer during JJA encompass a relatively wide range from 1 to 30 $\mathrm{m}^2\mathrm{s}^{-1}$.

The DJF impact on $Kv$ at the canopy layer height is shown in Fig. 13 and very similar patterns are seen when compared summer season, both qualitatively and quantitatively. The strongest impact is obtained for the two TKE based methods: DIRECT and MYJ reaching 15 to 30 $\mathrm{m}^2\mathrm{s}^{-1}$. On the other hand, a one order smaller impact is calculated for the CMAQ and YSU methods (up to 2 $\mathrm{m}^2\mathrm{s}^{-1}$). Similarly to the JJA impact, the ACM2 and OB70 methods lie in the middle range of the $Kv$-methods with the former one somewhat stronger. During both seasons, a few areas encounter statistically significant $Kv$

https://doi.org/10.5194/acp-2019-486
Preprint. Discussion started: 26 June 2019


Atmospheric Chemistry and Physics Discussions

decrease in the DIRECT and MYJ methods. This might be connected to the general wind stilling over large areas and the corresponding reduced TKE generation resulting in lower $Kv$ values, but this would require more analysis.

In order to understand the $Kv$ evolution during the day we plotted its diurnal cycle in Fig. 14 for Berlin. We are interested here not only on the urban canopy values, but on the impact on the whole $Kv$ profile (within the PBL) too and the absolute values from the URBAN model experiments are plotted too as contour layer. Regarding the absolute values, it is seen that largest $Kv$ are generated during early afternoon hours, in line with the expectations. The level of maximum $Kv$ is higher in JJA (about 150 - 600 m) than during DJF (100-500) and also higher for the 9 km simulation compared to 27 km one. The TKE based methods, DIRECT and MYJ produce higher values, reaching 200 $\mathrm{m^2 s^{-1}}$ for the DIRECT method and 120 $\mathrm{m^2 s^{-1}}$ for MYJ in JJA. The lowest $Kv$ values are calculated by the OB70 and YSU, reaching about 20 $\mathrm{m^2 s^{-1}}$ in summer. Winter $Kv$ values are much lower, as expected. It is also seen that $Kv$ values are usually larger for the 9 km simulation in both seasons. Here, the MYJ and DIRECT methods are exception with sightly higher values for the 27 km resolution. Somewhat distinct diurnal distribution is obtained with the ACM2 method. $Kv$ remain relatively large throughout the whole day and the maximum value is reached at much higher levels than for other methods, around 500–800 m. Turning our attention to the urban induced $Kv$ changes (shaded colors) it is seen, again, that the highest impact is obtained using the DIRECT and MYJ methods, reaching 100 $\mathrm{m^2 s^{-1}}$. It is also clear that the impact is higher during summer and stronger for the 9 km run for all methods. The highest impact occurs at comparable levels than the absolute values and consistently around late afternoon to early evening hours for each method. This means that the maximum of the impact is shifted by 3 to 6 hours later than the occurrence of the maximum absolute values. The smallest impact is simulated for the YSU and OB70 methods, reaching 10-20 $\mathrm{m^2 s^{-1}}$ at its maximum during afternoon/early evening hours.

In Fig. 15, the absolute $Kv$ values and the urban impact is shown for Prague for JJA in the same manner as for Berlin, only extended by the 3 km simulation. In general, both the absolute $Kv$ values as well as the impact is very similar to the impact over Berlin. The absolute eddy diffusion coefficient increases with increasing resolution and is, again, highest for the DIRECT a MYJ methods reaching 350 and 150 $\mathrm{m^2 s^{-1}}$, respectively. The lowest $Kv$ values are obtained when calculated by the YSU and OB70 methods (up to 20 $\mathrm{m^2 s^{-1}}$)). It is also clear, that at higher resolution, the maximum $Kv$ occurs at higher levels. Regarding the impact, there is a very clear increase when going into higher resolutions and the change is especially large between the 27km and 9 km resolutions.

During winter, Fig. 16, absolute $Kv$ values are, of course, smaller compared to summer ones, however one cannot conclude clearly an increase when turning to higher resolutions. E.g. for the DIRECT and MYJ methods, the 27 km results are higher than those obtained for the 9km and 3 km simulations. However, the supremacy of these two methods still holds producing vertical diffusivities up to 40–50 $\mathrm{m^2 s^{-1}}$ (MYJ being higher). Regarding the urban impact, the DIRECT and MYJ methods result in strongest change, however, in contrary to Berlin (or to the summer Prague results), the strongest impact is modeled over the 27 km domain while for other $Kv$ methods, the difference between individual resolution is not significant.

https://doi.org/10.5194/acp-2019-486
Preprint. Discussion started: 26 June 2019


Atmospheric Chemistry and Physics Discussions

### 3.3 Impact on the air-quality

The chemical changes, in particular the changes in the concentrations of $O_3$ and PM2.5 due to the simulated urban meteorological effects are presented here. This includes the effects of temperature, wind and vertical diffusivity changes, which where analyzed in the previous section. The effect of the urban induced modifications of humidity is included too, however, we showed in Huszar et al. (2018b) that the impact is negligible and the main contributors to the overall change are the modifications of the three meteorological parameters listed above. In accordance with Huszar et al. (2018b), we will distinguish different impacts based upon which urban meteorological perturbations are considered, e.g. the "t+q+uv-impact" means the combined impact of temperature-, humidity- and wind changes; the "kv-impact" stands for the chemical changes triggered by perturbed vertical eddy diffusion values only and the "t+q+uv+kv-impact" means the impact of all considered urban meteorological changed which, in this paper, will be equivalent with the "total-impact". We will start with the impact of enhanced turbulent transport which is the main focus of this paper.

#### 3.3.1 The effect of perturbed diffusivities

In Figures 12–16 we presented the range $Kv$ values perturbed by the introduction of urban surfaces and it was seen that this change covers two orders of magnitude (increases from a few $\mathrm{m^2 s^{-1}}$ to tens of $\mathrm{m^2 s^{-1}}$). Here, our attention moves to what range of perturbations of $O_3$ and PM2.5 concentrations this leads (i.e. the kv-impact is evaluated for individual $Kv$ methods).

*Ozone*

Fig. 17 presents the summer perturbation of surface concentrations of ozone due to the urban induced $Kv$ enhancement for the three resolutions and six $Kv$ methods. Ozone is increased in all cases ranging from 0.2 ppbv to 3 ppbv, as expected according to Huszar et al. (2018a). They showed that the main contributor to this increase is the reduced destruction due to turbulence enhanced vertical removal of NOx from the surface layer and the increased turbulent flux from the RL during night. The smallest increase is modeled by the CMAQ and YSU methods. At 27 km resolution, the largest effect is obtained using the DIRECT method, at 9 km the four remaining methods gives rather comparable impact for both cities. At 3 km resolution, the largest impact is seen for the ACM2 and OB70 methods. For Berlin, higher resolution leads to stronger impact for each method. For Prague, it is most often the 27 km resolution where the highest impact is modeled (expect YSU). In general, the impact over Berlin is stronger than over Prague.

The winter impact in Fig.18 is stronger than the summer one often reaching 4–5 ppbv. Here again, the smallest effect is obtained using the CMAQ and YSU methods. The strongest one is seen for DIRECT, MYJ and ACM2 for each resolution. It is also clear that higher resolution usually leads to smaller modeled impact.

To gain a more detailed insight into the range of kv-impacts, we also plotted the diurnal cycle of the vertical profile above both analyzed cities along with the absolute values. In Fig. 19, we present the results for Berlin for both seasons. Regarding the absolute values in JJA, values at higher levels are higher and this elevated maximum (usually around 200-500 m) "reaches" the surface as the usual early afternoon summer ozone maxima occur (about 40-50 ppbv). These are somewhat higher in the 9 km

https://doi.org/10.5194/acp-2019-486
Preprint. Discussion started: 26 June 2019


Atmospheric Chemistry and Physics Discussions

resolution. Turning our attention to the impact, a very clear maximum is seen near the surface during early evening reaching 6 ppbv while the effect is stronger for the 9 km resolution. This maximum is not visible only for the OB70 method at the 27 km resolution. Another striking feature is the ozone decrease up to -2 ppbv at higher levels (200-400 m) with maximum intensity coinciding with the maximum surface increase and slightly shifted compared to maxima of the absolute values. In general the impact (similarly to the absolute values) is more pronounced for the 9 km resolution and reaches higher levels. A secondary ozone maximum in the daily cycle is detectable during noon to evening at altitudes around 500-1500 m (higher altitudes at 9 km resolution) reaching 0.3-0.4 ppbv. During winter, the pattern of absolute values is much simpler with gradually increasing concentrations with increasing altitude with the expected weak afternoon maximum. The 9 km resolution profiles have usually lower values compared to 27 km ones, except near the surface when the ACM2 method provides higher values. The kv-impact on ozone is characterized with a clear increase at the surface model layer with a weak maximum during late afternoon up to 6 ppbv while the strongest effect is modeled for the DIRECT and ACM2 methods. The diurnal amplitude of the impact is much smaller than during JJA and is is clearly stronger for the 9 km resolution than for the 27 km one. The higher level ozone decrease is well seen (around 300-400 m; up to -2 ppbv reduction) and is much stronger for the 9 km resolution.

The pattern of the kv-impact on $O_3$ as well as that of the absolute values is very similar for Prague compared to Berlin, as seen in Fig. 20. The ozone increase is limited to the lowermost layers and there is again a clear early evening maximum reaching 5-6 ppbv. Also the impact reaches almost zero values during midday near the surface. The decrease at higher levels (200-400 m) with maximum during late afternoon/early evening is visible too and reaches -2 to -4 ppbv. Finally, the secondary maximum of ozone increase during noon hours at around 500-1500 m is visible too reaching 1 ppbv. The impact for the 3 km resolution seems to be the smallest, probably in connection with the fact that the absolute values are the smallest at this resolution too.

During winter over Prague, Fig. 21, both the absolute values and the kv-impact resembles the pattern seen for Berlin. The diurnal amplitude is much smaller for the impact with maxima usually around early evening and occasionally a weaker maximum is seen during morning hours for the DIRECT, ACM2, OB70 and MYJ methods. Again, the smallest impact is modeled for the CMAQ and YSU methods and the values for the 3 km resolution are below those for lower resolutions. The ozone decrease at higher altitudes (around 200-500 m) is detectable too, reaching -2 ppbv.

In summary, different $Kv$-methods lead to not only different average kv-impact on ozone values, but different vertical profiles and different shape of the daily cycle including the timing of the maximum value and occurrence of secondary maxima at higher altitudes.

*PM2.5*

Our attention now turns to the $\mathrm{PM2.5}$ changes and we first look at the changes in surface concentrations due to the kv-impact. The results for JJA and DJF are presented in Fig. 22 and Fig. 23, respectively. For summer and for Prague, there is a clear decrease of PM2.5 in line with the expectation of higher vertical turbulent removal (dispersion) of aerosol as well as their precursors (Huszar et al., 2018b). In general, the 27 km resolution produces stronger decrease up to -2 $\mu\mathrm{gm}^{-3}$, especially for the DIRECT, ACM2 and OB70 methods. For higher resolutions, these methods lead to largest impacts too (-1 to -2 $\mu\mathrm{gm}^{-3}$)

https://doi.org/10.5194/acp-2019-486
Preprint. Discussion started: 26 June 2019


Atmospheric Chemistry and Physics Discussions

while very weak impact is modeled using the CMAQ and YSU methods from -0.2 to -0.4 $\mu gm^{-3}$. A slightly different picture is obtained for the kv-impact for Berlin. While at 9 km resolution, the conclusions are very similar to the ones seen for Prague (decreases of PM2.5 of similar magnitude, ACM2 and OB70 providing the strongest impact), at 27 km resolution the impact is either a very small decrease (DIRECT and ACM2, up to -0.2 $\mu gm^{-3}$) or a slight increase up to 0.3 $\mu gm^{-3}$ for the rest of the methods. It is seen that there is a general increase of PM2.5 over large part of the analyzed region and this increase dominates the impact over Berlin. This increase is probably caused by the PM2.5 removed from the urban atmosphere (due to higher $Kv$ values) and transported to other regions where it causes an opposite effect.

During winter, the kv-impact leads to clear increase of PM2.5 concentrations for all resolutions, cities and methods. The strongest impact is seen for the DIRECT, ACM2 and MYJ methods peaking at -2 $\mu gm^{-3}$ while, again, the smallest impact is seen for the CMAQ and YSU methods (below -1 $\mu gm^{-3}$). It is also clear, that the impact calculated for lower resolutions is usually slightly stronger, especially over Prague.

In order to see, how the kv-impact on PM2.5 evolves during the day, we plotted on Fig. 24 the diurnal cycle of the impact of urban $Kv$ enhancement on the PM2.5 vertical profiles along with the absolute values. At the surface, the absolute values are higher during winter (18 $\mu gm^{-3}$) than during summer (up to 15 $\mu gm^{-3}$) as expected due to more stagnant meteorological conditions. However, at higher elevations summer concentrations are higher due to enhanced vertical transport. It is also clear that for the 9 km resolution, PM2.5 decreases with height slower than in the 27 km run, which is in line with the slightly stronger vertical mixing in the 9 km resolution compared to 27 km one (see Fig. 14). Further it is seen that $Kv$ methods giving stronger vertical turbulent diffusivities (e.g. DIRECT) result in lower near surface concentrations and vice versa (e.g. OB70), especially for summer. The diurnal cycle of the absolute values are characterized with clear maximum during morning hours and a minimum (especially in JJA) during afternoon. Looking at the kv-impact on PM2.5 concentrations, it is seen that the near surface values are characterized with decreases except the 27 km resolution values during JJA (in line with Fig. 22). At 9 km resolution during JJA, this decrease encompasses two peaks: a primary peak during afternoon reaching -1 $\mu gm^{-3}$ and a secondary peak during morning (up to -0.6 $\mu gm^{-3}$). The strongest impact is provided by DIRECT, ACM2 and OB70 methods as seen in the spatial figure above. At higher altitudes, the PM2.5 removed from the surface levels causes a positive impact "region" (at about 100–300 m) up to 0.3–0.4 $\mu gm^{-3}$ and occurring during afternoon. At 27 km however, this elevated maximum reaches the ground and leads to almost complete disappearance of surface decreases. During DJF, the two resolutions qualitatively behave in a very similar way. Both lead two a well pronounced surface PM2.5 decrease while it is stronger in the 9 km resolution (up to -2 to -3 $\mu gm^{-3}$). The DIRECT and ACM2 methods provide the largest impact. The double peak shape of the near surface impact is less clear or missing, instead, the kv-impact remain high from morning to evening hours (i.e. during daytime). The elevated increase of PM2.5 is more pronounced during the cold season and is, similarly to JJA, stronger over the 9 km domain, reaching 0.5–0.6 $\mu gm^{-3}$ at about 200–500 m.

For Prague, the JJA absolute values in Fig. 25 look quantitatively and qualitatively very similar to those over Berlin with peak values around 10-15 $\mu gm^{-3}$ during morning hours while higher values are modeled with $Kv$-methods producing lower $Kv$ values (e.g. OB70). The kv-impact manifests again as two maxima of the near surface PM2.5 decrease reaching -2 to -3 $\mu gm^{-3}$. The strongest impact is seen for the DIRECT, ACM2 and OB70 methods as seen for Berlin too. The elevated positive

https://doi.org/10.5194/acp-2019-486
Preprint. Discussion started: 26 June 2019


Atmospheric Chemistry and Physics Discussions

impact seen for Berlin is present here too and reaches 0.5–0.6 $\mu gm^{-3}$ with two maxima, one during morning hours and one during evening hours. In general, the impact over the 9 and 3 km resolution (up to -3 $\mu gm^{-3}$) is stronger than over the coarse 27 km domain (up to -1.5 $\mu gm^{-3}$).

Fig. 26 presents the absolute kv-values and the kv-impact for DJF for Prague, it is clear that the 9 and 3 km resolutions result in higher near surface concentrations and the vertical spread of the PM2.5 is stronger than for the 27 km domain. Regarding the impact, it reaches higher values in the 9 km and 3 km resolution and the maximum kv-impact is reached for DIRECT, ACM2 and OB70 methods (up to -3 $\mu gm^{-3}$ decrease) during daytime. For the 27 km resolution and for the YSU and CMAQ methods, the PM2.5 decrease is smaller (up to about -1 $\mu gm^{-3}$). Similar to Berlin, the PM2.5 increase and higher levels is evident too and is stronger for the 9 and 3 km resolutions. It occurs between 150–400 m and reaches 0.8-1 $\mu gm^{-3}$, especially for the DIRECT, ACM2 and OB70 methods.

### 3.3.2 The total urban impact

One of the most important questions to answer in this paper concerns the dominance of enhanced turbulence within the urban impact on air-quality via the urban meteorological effects. To answer this question, we evaluated the total- or the t+q+uv+kv-impact for both analyzed pollutant as the difference between the URB_t+q+uv+kv and NOURBAN model experiments for each resolution. As the NOURBAN model experiment is calculated using only the CMAQ $Kv$-method, the total-impact is given also only for this method. Here, based on short 1 month test simulations, we checked that the t-, q- and uv-impacts depend on the choice of the $Kv$ calculation weakly (in contrast with the kv-impact itself which is strongly dependent on the choice of the $Kv$ scheme).

Fig. 27 presents the total-impact of the urban meteorological changes on the mean surface concentrations of $O_3$ for each resolution and both seasons. Huszar et al. (2018a) predicted that near surface ozone should increase due to the increased removal (trubulent dispersion) of NOx from urban areas and thus reduced titration as well as due to enhanced turbulent transport from higher levels, although they pointed out that the overall effect is always a result of competitive impact of multiple influences. Indeed, in our results ozone usually increases too but the magnitude of the increase changes substantially across resolutions and it is different for the two cities. For Berlin, it reaches around 0.2–0.3 ppbv and 0.4–0.6 ppbv for the 27 and 9 km simulation, respectively. For Prague, increases are encountered for the 9 and 3 km resolution, reaching 0.3 and 0.8 ppbv, respectively. However, for the 27 km simulation, the overall urban impact turns to be negative (about -0.2 ppbv). During DJF, ozone increases over both cities, mostly for the 27 km resolution (reaching 0.8 ppbv). However, for Prague, in the 3 km resolution, $O_3$ decreases (up to -0.6 ppbv), in contrast with JJA. In order to see, whether the simulated total-impact is uniform during the day or it behaves qualitatively and quantitatively differently during different hours, we plotted further the diurnal cycle of this impact along with the absolute concentrations for both cities and seasons, as shown in Fig. 28. For JJA the absolute values (solid lines) are in line with the expectation with maximum during afternoon while the difference between the different resolutions is not greater than 6-8 ppbv (greatest differences in the daily maxima and nighttime values). The impact (dashed lines) is characterized with a clear main maximum during afternoon hours reaching up to 3 ppbv for Berlin, while it is less pronounced in the coarse resolution simulation. A secondary maximum is visible too during morning hours, especially for Prague. The

https://doi.org/10.5194/acp-2019-486
Preprint. Discussion started: 26 June 2019


Atmospheric Chemistry and Physics Discussions

minimum of the impact is encountered during early afternoon and here, the differences between the resolutions are very large for Prague ranging from -2 to 0 ppbv, explaining the overall negative impact of the urban canopy meteorological forcing on ozone in the previous figure. During winter, absolute ozone concentrations encounter two maxima, one during early morning and one during early afternoon. In winter, ozone titration is the dominant process in cities while ozone is transported here by turbulence from upper levels. The titration rate is highest when NOx emissions are peaking and this occurs in morning and later afternoon, putting the two ozone maxima in-between. In general, the 9 and 3 km resolution results in higher absolute ozone for this season, especially during nighttime. The total-impact is, again, characterized with a clear late-afternoon maximum reaching 2-3 ppbv and being strongest in the 27 km simulation. It is present also in the 3 km simulation for Prague, however, a negative peak forms here during morning (reaching -1.5 ppbv), which results in the overall negative impact on ozone seen in Fig.27.

The total-impact on PM2.5 surface concentrations is presented in Fig. 29. The impact is negative in all cases confirming the expectations that the effect of turbulent removal dominates (Huszar et al., 2018b), however the magnitude of the change varies greatly between the cities and resolutions. It reaches -1.5 to -2 $\mu\mathrm{gm}^{-3}$ for Prague in both summer and winter, and is strongest over the 27 km domain, while at 3 km, the decrease is only about -0.6 $\mu\mathrm{gm}^{-3}$. Over Berlin, the decrease is in the range of -0.4 to -1 $\mu\mathrm{gm}^{-3}$; in summer, it is slightly stronger over the 9 km run and in winter, the opposite holds.

The diurnal cycle of the absolute near surface PM2.5 concentrations as well as the total-impact over Berlin and Prague is presented in Fig. 30. A clear maximum occurs in the absolute values in summer during morning hours over both cities in line with the emission temporal evolution, while the difference between individual resolutions is within 5 $\mu\mathrm{gm}^{-3}$ and is highest during nighttime when the 27 km run produces the largest concentrations. Regarding the total-impact, in summer there is a clear negative peak during evening hours for both cities reaching -2 $\mu\mathrm{gm}^{-3}$. However, in the 3 km run this peak is less pronounced and reaches only about -0.6 $\mu\mathrm{gm}^{-3}$. Here, another peak is present during morning hours and this is seen also over the 27 and 9 km domains, especially for Berlin. During winter, absolute concentrations exhibit a main maximum during morning hours while especially for Prague, a secondary peak is present during evening hours, probably in connections with the diurnal cycle of the emissions. The diurnal cycle of the impact is very similar between individual resolutions and cities with one main peak during morning hours when the impact is the smallest (almost disappears over Berlin in the 9 km run). Later, the impact increases, depending on the resolution, during noon to afternoon hours, reaching -2 $\mu\mathrm{gm}^{-3}$, similar to the summer impact. Again, the smallest impact is modeled over the 9 km resolution (about -1 $\mu\mathrm{gm}^{-3}$).

In summary, when comparing the individual resolutions, it is clear that the total-impact for both ozone and PM2.5 can vary largely, in both quantitative and qualitative sense. Further it is evident, that the kv-impact (evaluated in the previous section) will add further uncertainty to the results as its spread is even larger than the spread seen in the total-impact due to different resolutions (bear in mind that the kv-impact represents a major component of the total impact). Remember, that the total-impact was evaluated using the CMAQ method. This resulted in one of the smallest kv-impacts. Even as such, it clearly dominates the total-impact. Consequently, using other $Kv$ methods would lead to even stronger total-impact (increase of ozone and decrease of PM2.5) and thus confirms the dominance of the changes in vertical turbulent transport among other components of the urban meteorological forcing.

https://doi.org/10.5194/acp-2019-486
Preprint. Discussion started: 26 June 2019


Atmospheric Chemistry and Physics Discussions

## 4 Discussion and conclusions

Results suggest a clear overestimation of winter temperatures in RegCM along with a precipitation overestimation. Previously, Giorgi et al. (2012) reported this positive bias too using the same PBL scheme (UW scheme). Along with the positively biased winter temperatures this suggest that the heat removal from the surface towards higher levels is probably underestimated (in contrast with the older HOL scheme) and this leads to higher surface temperatures. Large positive rain bias was showed also in Huszar et al. (2016b) and they attributed it to overestimation of cloudiness which in winter, can lead to positive temperature bias (reduced radiative cooling). In summer, the results are more mixed but the model stays within a reasonable range compared to observation.

The comparison of modeled concentrations with observations showed several model deficiencies. For ozone, it is especially the strong overestimation of the nighttime values (while daytime peaks are reasonably captured), this leads to underestimation of the diurnal amplitude significantly. This was commonly encountered in regional climate chemistry studies (Zanis et al., 2011; Huszar et al., 2016a; Karlický et al., 2017). Zanis et al. (2011) found that night-time ozone values are captured in the model (they used CAMx too) with less accuracy than daytime ones and argue that this is caused by more stable conditions when ozone values are more sensitive to the vertical profiles of meteorological variables, emissions and the precursor concentrations. It is clear that in future, more emphasis should be given on processes determining nighttime surface ozone, as improving the nighttime model accuracy will yield more reasonable starting point for the development of daytime ozone (Wong and Stutz, 2010) and an overall better model performance. Consequently, the monthly ozone averages are overestimated. Higher model ozone may suggest that some of the urban impacts on ozone may be slightly overestimated, assuming that the impact increases with increasing absolute values. It is also evident from the results that higher resolutions did not bring substantial improvement to model accuracy (except daily ozone maxima are captured with a higher accuracy in the 3 km model runs). The same conclusion as recently stated by Falasca and Curci (2018), who applied WRF over Italy at similar (cascading) domain resolutions. It also evident from the absolute values of concentrations in the ozone diurnal cycle figures, that $Kv$ methods produce higher diffusivities (compared to the default one) result in higher ozone values (e.g. the TKE based methods), which is due to higher $\mathrm{NOx}$ turbulent removal in cities and therefore lower ozone titration. This means that the positive ozone bias will be even higher. This however does not mean that these methods are erroneous as the model bias has in general multiple reasons (inaccurate diurnal profile of emissions, biased nighttime chemistry etc.) rather than caused by one particular process (vertical eddy diffusion).

Regarding the PM2.5, the most important model shortcoming is the strong underestimation of observed values during winter, especially over urban stations. On the other hand, overestimation occurs in summer, especially for the 27 km and 9 km domains. Many stations from western Europe were included in the validation and these showed systematic model overestimation also in Huszar et al. (2018b) and overweight the underestimation seen for other central European countries, especially Czech republic, which encompasses the whole 3 km domain. Note that the emission data used in this study is basically a new version of that used in the former study and differs only slightly. The REZZO/ATEM emissions used for Czech republic are also quantitatively very similar to the TNO data over the this country too. Huszar et al. (2016a), using similar model resolution and emission data,

https://doi.org/10.5194/acp-2019-486
Preprint. Discussion started: 26 June 2019


Atmospheric Chemistry and Physics Discussions

showed similar large DJF underestimations of PM2.5 and attributed it to underestimated nitrate aerosol and black/organic carbon. Myhre et al. (2006) and Schaap et al. (2004) encountered similar negative bias for these aerosol components. Further we see that, that using other $kv$ calculation method which produce stronger diffusivities will results in higher turbulent removal of PM2.5 from near the surface resulting in more pronounced negative bias. However, similar to the case of ozone, this does not imply that these "stronger" $Kv$ schemes are wrong as, again, the model bias has multiple components (and here is caused most probably bias in the secondary aerosol formation). In such cases, improving model physics can often lead reduced model accuracy.

In summary, a weak sensitivity of modeled concentrations to the resolution of the driving meteorological as well as CTM is seen as concluded earlier by Markakis et al. (2015) who performed similar climate driven air-quality simulations over Paris (France). Indeed, the largest uncertainity of modeled concentrations is associated with emissions, especially over urban areas (Aleksankina et al., 2019), however, recall that in our case, emission where kept constant and the uncertainty to the representation of urban boundary layer was analyzed only.

The average urban impact on temperature is very similar to the values presented in Huszar et al. (2018a) who, for the two analyzed cities (Berlin and Prague), encountered increases up to 1.5–2° C. The diurnal variation of the impact shows also large similarities in both quantitative and qualitative sense, when the maximum impact occurs around late evening. The urban impact on temperature is consistent with previous observation- (Gaffin et al., 2008) and model based studies (Pichierri et al., 2012; Giannaros and Melas, 2012; Struzewska and Kaminski, 2012) while Sarrat et al. (2006) simulated somewhat later timing of the maximum urban impact. Our simulations, extended to DJF, suggest that the magnitude of the impact remain similarly high during winter and here probably the effects of anthropogenic heat dominate over the radiative and thermal effects associated with radiation trapping (Karlický et al., 2018; Varentsov et al., 2018). Although increased resolution results in spatially more detailed impact with maximum temperature impact concentrated to the city center (seen especially for Prague in the 3 km run), there is no systematic effect of the choice of resolution. It strongly depends on how the model grid covers a particular city and if the city center matches a grid point (Prague) or it lies in-between (Berlin). This suggest that efforts should be made to adapt the grid to the geographic location of city centers which is best achieved by choosing multiple disjunct nested domains under the parent grids (e.g. as in Wang et al., 2012).

The impact on average wind speed with values up to -2 $\mathrm{ms}^{-1}$ decreases match previous studies too. E.g. Struzewska and Kaminski (2012) simulated similar decreases for central European cities, but Chinese cities in Zhu et al. (2017) encounter comparable decreases as well. Compared to the decreases in Huszar et al. (2018a), up to -1 $\mathrm{ms}^{-1}$, our results suggest that in case of wind, higher resolutions bring stronger impact. Indeed, the 27 km and the 9 km impacts are always less than the 3 km result for Prague. This indicates that higher resolution yield stronger peak wind modifications in city centers. A sudden decrease (in absolute sense) of the wind-impact during evening hours is visible in our simulations too and is probably connected to the evening PBL transition (Lapworth, 2003). The wind impact during winter turned to be somewhat larger than summer, which is connected to more stable stratification when less turbulence is present (see further) and less momentum is transfered to the surface from above the PBL. The timing of both the minimum and maximum urban wind speeds (as well as those of temperature) is in very good agreement with Zhang and Zheng (2004).

https://doi.org/10.5194/acp-2019-486
Preprint. Discussion started: 26 June 2019


Atmospheric Chemistry and Physics Discussions

Our results suggest large sensitivity of the modeled vertical eddy diffusivities on the choice of the methods for its calculation and the same is true for the urban impact. Near surface $Kv$ modifications range two orders of magnitude from 0.5 to as much as 30 $\mathrm{m^2 s^{-1}}$. The impact over higher levels cover even wider range of values from 1 up to 100 $\mathrm{m^2 s^{-1}}$. The TKE based methods systematically generate higher $Kv$ values, this is in line with Kim et al. (2015) who compared a improved version of MYJ used here and the YSU scheme. They concluded that MYJ generate stronger vertical mixing at about 400–500 m above the surface than the YSU scheme, although the depth of the PBL was larger in YSU in their simulations. Our $Kv$ values for the CMAQ method are in good agreement with the values of Huszar et al. (2018a) calculated according to the same method. Kim et al. (2015) predicted $Kv$ increase due to application of urban canopy scheme up to 100 $\mathrm{m^2 s^{-1}}$, same as in our study and the height of the maximum increase well coincides with our results too. In ENVIRON (2011), OB70 and YSU methods generated the smallest $Kv$s too, in line with our results. They however predicted $Kv$ values for the MYJ methods comparable to CMAQ (and comparable to our CMAQ values), in contrary to our results. These could suggest that the turbulent kinetic energy (TKE), from which $Kv$ is derived, is somewhat overestimated in our RegCM simulations. Resolution seems to have rather minor impact on the result near the surface. However, finer resolution results in stronger impact at higher elevations. This seems to be true for both the absolute diffusivities as well as for the urban impact. Regarding the difference between winter and summer, DJF absolute $Kv$ values are lower, as expected from the more frequent stable stratification. The impact on $Kv$ at higher levels are stronger in summer, however at the surface the difference between summer and winter is rather small. The maximum $Kv$ impact is simulated in all diffusion schemes during early evening. This is related to the evening PBL transition when urban PBL height decrease more slowly than the rural ones resulting in relatively large urban-rural difference and hence large impact on $Kv$ (Pal et al., 2012).

The simulated changes in the vertical eddy diffusion coefficient alone led to ozone increases as expected from previous studies of Sarrat et al. (2006); Kim et al. (2015). NOx is removed from the surface layer more efficiently over urbanized areas leading to reduced ozone titration while at the same time the increased transport from the residual layer during nighttime is contributing too, as showed by Huszar et al. (2018a). They used the CMAQ method for $Kv$ calculation, and simulated (for JJA) a higher ozone increase up to 3 and 2 ppbv over Berlin and Prague, respectively, compared to our CMAQ results of about 1.5 and 0.8 ppbv for Berlin and Prague. Higher kv-impact on ozone, up to 4 ppbv is simulated with the TKE based methods, but comparable magnitude is achieved also with the ACM2 and OB70 approaches. It is not clear weather higher resolution lead to systematic change of the urban core kv-impact, often the middle resolution (9 km) exhibit the largest value. Interestingly, the kv-impact for OB70 is one of the strongest while the urban induced $Kv$ modifications were at the low end in case of this methods. This is also true for the ACM2 method for which the $Kv$ modification where far not the strongest however this propagated to almost the strongest impact on near surface ozone. The impact during winter is somewhat stronger than in summer, maybe due to more important role of the reduced titration in winter, when NOx levels are higher. Again, the CMAQ and YSU methods generate weakest ozone changes. In summary, the simulated range of $Kv$ changes of about 0.5 to 30 $\mathrm{m^2 s^{-1}}$ propagated to a range of the kv-impact near the surface of about 0.6 to 4 ppbv. The vertical profile of ozone changes further showed decreases at higher levels. This is probably due to NOx removed from the surface causing titration at higher levels but the increased transport from RL removing ozone there can contribute too. Zhu et al. (2015) showed that in urban plumes,

https://doi.org/10.5194/acp-2019-486
Preprint. Discussion started: 26 June 2019


Atmospheric Chemistry and Physics Discussions

ozone is increased in upper boundary and decreased in the lower one. Our result exhibit a small increase of ozone at higher levels and the mentioned decrease often extends to the lower boundary layer, putting our results in line with theirs. The range of elevated ozone decreases due to different $Kv$ methods is relatively large, spanning from -0.4 to -2 ppbv.

The response of the near surface PM2.5 concentrations to urban enhanced vertical turbulent transport shows predominantly decreases as the process of increased eddy diffusion removal dominates (Zhu et al., 2017; Kim et al., 2015). Huszar et al. (2018b) however showed, that individual aerosol components react differently to increased eddy transport and secondary aerosols can even increase slightly. However, in their study, primary aerosol decrease strongly shaping the total PM2.5 response. Our results suggest PM2.5 decrease from a few -0.1 $\mu\mathrm{gm}^{-3}$ up to -1 $\mu\mathrm{gm}^{-3}$ in summer and even stronger decrease (up to -2 $\mu\mathrm{gm}^{-3}$) in winter, which is - at least for summer - quantitatively close to Huszar et al. (2018b) who simulated summer decreases for Berlin and Prague up to -2 and -1 $\mu\mathrm{gm}^{-3}$, respectively. The decreases due to urban induced $Kv$ enhancement in Kim et al. (2015) are somewhat larger, but this can be due to different city chosen (Paris). Our results indicate that in connection with $Kv$ enhancement, even increases can occur. This is probably due to the fact, that the aerosol removed from the surface level to the upper ones is transported to other regions where it deposits back to lower levels overweighting the turbulence enhanced local reduction. This effect is expected to be strong over larger domain where the simulation allows the aerosol to be transported to larger distances. Indeed, our 27 km domain results show some PM2.5 increase, especially over rural areas but also for Berlin. Our results further showed that the winter PM2.5 decreases are larger, which is in line with the fact that the winter $Kv$ increase are higher too. Comparing the individual $Kv$ methods, it is seen that the strongest impact is simulated by the ACM2 scheme, but the OB70 and the TKE based schemes are comparably strong too. On the other hand, the default CMAQ scheme generates much weaker impact along with the YSU scheme. Kim et al. (2015) concluded too that the MYJ scheme resulted in larger impact on PM than the YSU. We also found that during summer the strongest impact is modeled during afternoon/evening hours reaching -3 $\mu\mathrm{gm}^{-3}$, in line with Huszar et al. (2018b). The choice of the $Kv$ methods however strongly determines the shape of the diurnal cycle of the impact, especially in summer.

The total urban impact (i.e. the combined impact of temperature-, humidity-, wind- and turbulence) exhibited a relatively large range of values for ozone from -0.6 to 0.8 ppbv, depending on the resolution and season. This underlines the fact, that the total-impact encompasses multiple components that act simultaneously and have opposite sign (Huszar et al., 2018a). This include decrease due to increased $\mathrm{NO} + \mathrm{O_3} \rightarrow \mathrm{NO_2}$ reaction, decrease due to increased dry deposition, decrease due to increased titration caused by decreased wind and finally, increase due to vertical turbulent removal of NOx from the near surface where it causes titration. Over Prague, the wind and the temperature impact in winter was evaluated to be relatively large, while the CMAQ impact on $Kv$ small. As the total-impact was evaluated only for this $Kv$ method, this suggest that decreases due to increased temperature and decreased wind speeds will be strong and indeed, they apparently overweighted the impact of enhanced turbulence leading to concentration decrease, especially over the fine resolution domain. However, when we compare this results to the much stronger kv-impact gained by other $Kv$ methods, we clearly see that using them would turn to impact into positive making the turbulence changes again a dominant factor shaping the total-impact. We can conclude here, that the vertical eddy diffusion is a dominant factor that determines the impact of urban canopy forcing on ozone, however

https://doi.org/10.5194/acp-2019-486
Preprint. Discussion started: 26 June 2019


Atmospheric Chemistry and Physics Discussions

there is relatively large uncertainity given the way how $Kv$ values are calculated and under certain conditions this dominance is not clear or can be even slightly overweighted by opposite effects.

In case of the total impact on PM2.5, the dominance of enhanced turbulence is clear for each resolution, city and season, although the magnitude covers a wide range, from a few -0.1 $\mathrm{m^2 s^{-1}}$ up to -2 $\mathrm{m^2 s^{-1}}$. Here, the counteracting effect is the decreased windspeed which reduces the dilution into larger scales and leads to PM2.5 increases (Huszar et al., 2018b). As already said, the CMAQ methods was used to calculate the total impact and again, the PM2.5 changes due to kv-impact calculated using this method turned to be one of the smallest. We can conclude thus here that using other methods would lead to even larger decreases of PM2.5 due to the total urban impact, confirming the dominance of enhanced vertical eddy transport over urban areas.

In summary, our results confirm that turbulence is a prominent factor that determines the impact of urban canopy meteorological forcing on the urban air-quality. In case of ozone, it leads to increased concentrations while PM2.5 responses with decreases. This holds for both summer and winter season. Finally, model resolution seems to play rather a minor role and the effect of urban induced modification of vertical eddy diffusion is dominant in both coarse and high resolution model experiments. Our study demonstrates the dominant role of turbulent transport of pollutants above urban areas and stresses the need for further investigation how variation of urban land-use (within urban mitigation and adaptation) influence the pollutant transport from the urban canopy.

*Code and data availability.* The model RegCM4.6 is freely available for public under https://gforge.ictp.it/gf/download/frsrelease/257/1784/RegCM-4.6.1.tar.gz. CAMx version 6.50 is available under http://www.camx.com/download/default.aspx. The RegCM2CAMx meteorological preprocessor used to convert RegCM outputs to CAMx inputs is available upon request from the main author. The complete model configuration and all the simulated data (3D for meteorological variables, 3D for ozone and PM2.5 and 2D for other chemical species) used for the analysis are placed on the Data storage center of the Czech CESNET service (https://www.cesnet.cz/e-infrastruktura-3/data-storage/?lang=en) and counts about 40 TB. These data are available upon request from the main author.

*Author contributions.* PH provided the scientific idea and the design of the model experiments, and led the writing of the paper; PH, JK and MB assisted in maintaining the models and performing the runs, JD, PP, TN and KS contributed to the evaluation of the results, TH, MZ and JD helped with writing the paper

*Competing interests.* The authors declare that they have no conflict of interest.

*Acknowledgements.* This work has been funded by the Czech Science Foundation (GACR) project No. 19-10747Y and partly by the projects OP-PPR (Operation Program Prague – Pole of Growth)

https://doi.org/10.5194/acp-2019-486
Preprint. Discussion started: 26 June 2019


Atmospheric Chemistry and Physics Discussions

CZ.07.1.02/0.0/0.0/16_040/0000383 “URBI PRAGENSI - Urbanization of weather forecast, air quality prediction and climate scenarios for Prague” and by projects PROGRES Q47, Q16 and SVV 2017 – Programmes of Charles University. We further acknowledge the TNO MACC-III emissions dataset, the Air Pollution Sources Register (REZZO) dataset issued by the Czech Hydrometeorological Institute and the ATEM Traffic Emissions dataset provided by ATEM (Studio of ecological models). We also would like to acknowledge the E-OBS dataset from the EU-FP6 project ENSEMBLES (http://ensembles-eu.metoffice.com) and the data providers of AirBase European Air Quality data (http://www.eea.europa.eu/data-and-maps/data/aqereporting-1). Finally, we acknowledge the IT4Innovations National Supercomputing Center in Ostrava (Czech republic) who provided the computational resources (internal call OPEN-13-13) needed to perform the model experiments.

https://doi.org/10.5194/acp-2019-486
Preprint. Discussion started: 26 June 2019


Atmospheric Chemistry and Physics Discussions

## References

Aleksankina, K., Reis, S., Vieno, M., and Heal, M. R.: Advanced methods for uncertainty assessment and global sensitivity analysis of an Eulerian atmospheric chemistry transport model, Atmos. Chem. Phys., 19, 2881-2898, https://doi.org/10.5194/acp-19-2881-2019, 2019.

Baklanov, A., Molina, L. T., and Gauss, M.: Megacities, air quality and climate, Atmos. Environ., 126, 235-249, http://dx.doi.org/10.1016/j.atmosenv.2015.11.059., 2016.

Barnes, M. J., Brade, T.K., MacKenzie, A.R., Whyatt, J.D., Carruthers, D.J., Stocker, J., Cai, X. and Hewitt, C.N.: Spatially-varying surface roughness and ground-level air quality in an operational dispersion model, Environ. Pollution, 185, 44–51, https://doi.org/10.1016/j.envpol.2013.09.039, 2014.

Belcher, S.E., Coceal, O., Goulart, E.V. Rudd, A.C. and Robins, A. G.: Processes controlling atmospheric dispersion through city centres, J. Fluid Mech., 763, 51-81, 2015.

Benešová, N., Belda, M., Eben, K., Geletič, J., Huszár, P., Juruš, P., Krč, P., Resler, J. and Vlček, O.: New open source emission processor for air quality models, In Sokhi, R., Tiwari, P. R., Gállego, M. J., Craviotto Arnau, J. M., Castells Guiu, C. and Singh, V. (eds) Proceedings of Abstracts 11th International Conference on Air Quality Science and Application, doi: 10.18745/PB.19829. (pp. 27). Published by University of Hertfordshire. Paper presented at Air Quality 2018 conference, Barcelona, 12-16 March, 2018.

van den Besselaar, E.J.M., Haylock, M. R., van der Schrier, G., and Klein Tank, A. M. G.: A European Daily High-resolution Observational Gridded Data set of Sea Level Pressure, J. Geophys. Res., 116, D11110, doi:10.1029/2010JD015468, 2011.

Butler, T. M., Stock, Z. S., Russo, M. R., Denier van der Gon, H. A. C., and Lawrence, M. G.: Megacity ozone air quality under four alternative future scenarios, Atmos. Chem. Phys., 12, 4413–4428, doi:10.5194/acp-12-4413-2012, 2012.

Byun, D. W. and Ching, J. K. S.: Science Algorithms of the EPA Model-3 Community Multiscale Air Quality (CMAQ) Modeling System. Office of Research and Development, U.S. EPA, North Carolina, 1999.

Bretherton, C. S., McCaa, J.R. and Grenier, H.: A New Parameterization for Shallow Cumulus Convection and Its Application to Marine Subtropical Cloud-Topped Boundary Layers. Part I: Description and 1D Results, Mon. Weather Rev., 132, 864-882, 2004.

Chen, B., Yang, S., Xu, X.D. and Zhang, W.: The impacts of urbanization on air quality over the Pearl River Delta in winter: roles of urban land use and emission distribution, Theor. Appl. Climatol., 117, 29–39, 2014.

89–90, 212–221, 2016.

Dawson, J. P., Adams, P. J., and Pandis, S. N.: Sensitivity of PM2.5 to climate in the Eastern US: a modeling case study, Atmos. Chem. Phys., 7, 4295-4309, https://doi.org/10.5194/acp-7-4295-2007, 2007.

Emmons, L. K., Walters, S., Hess, P. G., Lamarque, J.-F., Pfister, G. G., Fillmore, D., Granier, C., Guenther, A., Kinnison, D., Laepple, T., Orlando, J., Tie, X., Tyndall, G., Wiedinmyer, C., Baughcum, S. L., and Kloster, S.: Description and evaluation of the Model for Ozone and Related chemical Tracers, version 4 (MOZART-4), Geosci. Model Dev., 3, 43-67, https://doi.org/10.5194/gmd-3-43-2010, 2010.

ENVIRON, Dallas-Fort Worth Modeling Support: Improving the Representation of Vertical Mixing Processes in CAMx – Final Report, ENVIRON International Corporation, Novato, California, 2011.

ENVIRON, CAMx User's Guide, Comprehensive Air Quality model with Extentions, version 6.50, www.camx.com, Novato, California, 2018.

Falasca, S. and Curci, G.: High-resolution air quality modeling: Sensitivity tests to horizontal resolution and urban canopy with WRF-CHIMERE, Atmos. Environ., 187, 241-254, https://doi.org/10.1016/j.atmosenv.2018.05.048, 2018.

https://doi.org/10.5194/acp-2019-486
Preprint. Discussion started: 26 June 2019


Atmospheric Chemistry and Physics Discussions

Fallmann, J., Forkel, R., and Emeis, S.: Secondary effects of urban heat island mitigation measures on air quality, Atmos. Environ., 25, 199–211, 2016.

Flagg, D. D. and Taylor, P. A.: Sensitivity of mesoscale model urban boundary layer meteorology to the scale of urban representation, Atmos. Chem. Phys., 11, 2951–2972, https://doi.org/10.5194/acp-11-2951-2011, 2011.

Folberth, G. A., Butler, T. M., Collins, W. J., and Rumbold, S. T.: Megacities and climate change – A brief overview, Environ. Pollut., 203, 235–242, http://dx.doi.org/10.1016/j.envpol.2014.09.004, 2015.

Gaffin, S. R., Rosenzweig, C., Khanbilvardi, R., Parshall, L., Mahani, S., Glickman, H., Goldberg, R., Blake, R., Slosberg, R. B., and Hillel, D.: Variations in New York City's urban heat island strength over time and space, Theor. Appl. Climatol., 94, 1–11, https://doi.org/10.1007/s00704-007-0368-3, 2008.

Ganbat, G., Baik, J. J. and Ryu, Y. H.: A numerical study of the interactions of urban breeze circulation with mountain slope winds, Theor. App. Clim., 120(1-2), 123–135, 2015.

Giannaros, T. M. and Melas, D.: Study of the urban heat island in a coastal Mediterranean city: the case study of Thessaloniki, Greece, Atmos. Res., 118, 103–120, https://doi.org/10.1016/j.atmosres.2012.06.006, 2012.

Giorgi, F., Coppola, E., Solmon, F., Mariotti, L., Sylla, M., Bi, X., Elguindi, N., Diro, G. T., Nair, V., Giuliani, G., Cozzini, S., Guettler, I., O'Brien, T. A., Tawfi, A. B., Shalaby, A., Zakey, A., Steiner, A., Stordal, F., Sloan, L., and Brankovic, C.: RegCM4: model description and preliminary tests over multiple CORDEX domains, Clim. Res., 52, 7–29, 2012.

van der Gon, H. D., Hendriks, C., Kuenen, J., Segers, A. and Visschedijk, A.: Description of current temporal emission patterns and sensitivity of predicted AQ for temporal emission patterns. EU FP7 MACC deliverable report D_D-EMIS_1.3, http://www.gmes-atmosphere.eu/documents/deliverables/d-emis/MACC_TNO_del_1_3_v2.pdf, 2011.

Grenier, H. and Bretherton C. S.: A moist PBL parameterization for large scale models and its application to subtropical cloud-topped marine boundary layers, Mon. Weather Rev., 129, 357-377, 2001.

Guenther, A. B., Jiang, X., Heald, C. L., Sakulyanontvittaya, T., Duhl, T., Emmons, L. K., and Wang, X.: The Model of Emissions of Gases and Aerosols from Nature version 2.1 (MEGAN2.1): an extended and updated framework for modeling biogenic emissions, Geosci. Model Dev., 5, 1471-1492, https://doi.org/10.5194/gmd-5-1471-2012, 2012.

Hao, L., Huang, X., Qin, M., Liu, Y., Li, W. and Sun, G.: Ecohydrological processes explain urban dry island effects in a wet region, southern China, Water Resour. Res., 54, 6757-6771. https://doi.org/10.1029/2018WR023002, 2018.

Hidalgo, J., Masson, V., and Gimeno, L.: Scaling the Daytime Urban Heat Island and Urban-Breeze Circulation, J. Appl. Meteorol. Clim., 49, 889–901, 2010.

Holtslag, A. A. M., de Bruijn, E. I. F., and Pan, H.-L.: A high resolution air mass transformation model for shortrange weather forecasting, Mon. Wea. Rev., 118, 1561–1575, 1990.

Hong, S., Noh, Y. and Dudhia, J.: A New Vertical Diffusion Package with an Explicit Treatment of Entrainment Processes, Mon. Wea. Rev., 134, 2318-2341, https://doi.org/10.1175/MWR3199.1, 2006.

Huszar, P., Juda-Rezler, K., Halenka, T., Chervenkov, H. and others: Effects of climate change on ozone and particulate matter over Central and Eastern Europe, Clim. Res. 50, 51-68, 2011, doi:10.3354/cr01036

Huszar, P., Miksovsky, J., Pisoft, P., Belda, M., and Halenka, T.: Interactive coupling of a regional climate model and a chemistry transport model: evaluation and preliminary results on ozone and aerosol feedback, Clim. Res., 51, 59–88, doi:10.3354/cr01054, 2012.

https://doi.org/10.5194/acp-2019-486
Preprint. Discussion started: 26 June 2019




Huszar, P., Teyssedre, H., Michou, M., Voldoire, A., Olivié, D. J. L., Saint-Martin, D., Cariolle, D., Senesi, S., Salas Y Melia, D., Alias, A., Karcher, F., Ricaud, P., and Halenka, T.: Modeling the present and future impact of aviation on climate: an AOGCM approach with online coupled chemistry, Atmos. Chem. Phys., 13, 10027–10048, doi:10.5194/acp-13-10027-2013, 2013.

Huszar, P., Halenka, T., Belda, M., Zak, M., Sindelarova, K., and Miksovsky, J.: Regional climate model assessment of the urban land-surface forcing over central Europe, Atmos. Chem. Phys., 14, 12393-12413, doi:10.5194/acp-14-12393-2014, 2014.

Huszar, P., Belda, M., and Halenka, T.: On the long-term impact of emissions from central European cities on regional air quality, Atmos. Chem. Phys., 16, 1331–1352, doi:10.5194/acp-16-1331-2016, 2016a.

Huszár, P., Belda, M., Karlický, J., Pišoft, P., and Halenka, T.: The regional impact of urban emissions on climate over central Europe: present and future emission perspectives, Atmos. Chem. Phys., 16, 12993-13013, doi:10.5194/acp-16-12993-2016, 2016b.

Huszar, P., Karlický, J., Belda, M., Halenka, T. and Pisoft, P.: The impact of urban canopy meteorological forcing on summer photochemistry, Atmos. Environ., 176, 209-228, https://doi.org/10.1016/j.atmosenv.2017.12.037, 2018a.

Huszar, P., Belda, M., Karlický, J., Bardachova, T., Halenka, T., and Pisoft, P.: Impact of urban canopy meteorological forcing on aerosol concentrations, Atmos. Chem. Phys., 18, 14059-14078, https://doi.org/10.5194/acp-18-14059-2018, 2018b.

Im, U., Markakis, K., Poupkou, A., Melas, D., Unal, A., Gerasopoulos, E., Daskalakis, N., Kindap, T., and Kanakidou, M.: The impact of temperature changes on summer time ozone and its precursors in the Eastern Mediterranean, Atmos. Chem. Phys., 11, 3847–3864, doi:10.5194/acp-11-3847-2011, 2011b.

Im, U. and Kanakidou, M.: Impacts of East Mediterranean megacity emissions on air quality, Atmos. Chem. Phys., 12, 6335–6355, doi:10.5194/acp-12-6335-2012, 2012.

Jacobson, M. Z., Nghiem, S. V., Sorichetta, A., and Whitney, N.: Ring of impact from the mega-urbanization of Beijing between 2000 and 2009, J. Geophys. Res., 120(12), 5740-5756, https://doi.org/10.1002/2014JD023008, 2015.

Jackson, T. L., Feddema, J. J., Oleson, K. W., Bonan, G. B., Bauer, J. T.: Parameterization of Urban Characteristics for Global Climate Modeling. Ann. Assoc. Am. Geogr. 100, 848–865, doi:10.1080/00045608.2010.497328 , 2010.

Janjic, Z. I.: The step-mountain Eta coordinate model: Further developments of the convection, viscous layer, and turbulence closure schemes, Mon. Wea. Rev., 122, 927-945, 1994.

Janssen, R. H. H., Tsimpidi, A. P., Karydis, V. A., Pozzer, A., Lelieveld, J., Crippa, M., Prévôt, A. S. H., Ait-Helal, W., Borbon, A., Sauvage, S. and Locoge, N.: Influence of local production and vertical transport on the organic aerosol budget over Paris, J. Geophys. Res., 122(15), 8276-8296, https://doi.org/10.1002/2016JD026402, 2017.

Juda-Rezler, K., Reizer, M., Huszar, P., Krueger, B., Zanis, P., Syrakov, D., Katragkou, E., Trapp, W., Melas, D., Chervenkov, H., Tegoulias, I., and Halenka, T.: Modelling the effects of climate change on air quality over central and Eastern Europe: concept, evaluation and projections, Clim. Res., 53, 179–203, doi: 10.3354/cr01072, 2012.

Karlický, J., Huszár, P. and Halenka, T.: Validation of gas phase chemistry in the WRF-Chem model over Europe, Adv. Sci. Res., 14, 181-186, https://doi.org/10.5194/asr-14-181-2017, 2017.

Karlický, J., Huszár, P., Halenka, T., Belda, M., Žák, M., Pišoft, P., and Mikšovský, J.: Multi-model comparison of urban heat island modelling approaches, Atmos. Chem. Phys., 18, 10655-10674, doi:10.5194/acp-18-10655-2018, 2018.

Kiehl, J., Hack, J., Bonan, G., Boville, B., Breigleb, B., Williamson, D., and Rasch, P.: Description of the NCAR Community Climate Model (CCM3), National Center for Atmospheric Research Tech Note NCAR/TN-420 + STR, NCAR, Boulder, CO, 1996.

Kim, Y, Sartelet, K., Raut, J.-Ch., and Chazette, P.: Influence of an urban canopy model and PBL schemes on vertical mixing for air quality modeling over Greater Paris, Atmos. Environ., 107, 289–306, doi:10.1016/j.atmosenv.2015.02.011, 2015

https://doi.org/10.5194/acp-2019-486
Preprint. Discussion started: 26 June 2019


Atmospheric Chemistry and Physics Discussions

Kuenen, J. J. P., Visschedijk, A. J. H., Jozwicka, M., and Denier van der Gon, H. A. C.: TNO-MACC II emission inventory; a multi-year (2003–2009) consistent high-resolution European emission inventory for air quality modelling, Atmos. Chem. Phys., 14, 10963-10976, https://doi.org/10.5194/acp-14-10963-2014, 2014.

Květoň, V. and Žák, M.: New climate atlas of Czechia, Stud. Geophys. Geod., 51, 345–349 , 2007.

Lawrence, D. M., Oleson, K. W., Flanner, M. G., Thornton,P. E., Swenson, S. C., Lawrence, P. J., Zeng, X., Yang, Z.-L., Levis, S., Sakaguchi, K., Bonan, G. B. and Slater, A.G.: Parameterization improvements and functional and structural advances in version 4 of the Community Land Model. J. Adv. Model. Earth Sys., 3, DOI: 10.1029/2011MS000045, 2011.

Lee, S.-H., Kim, S.-W., Angevine, W. M., Bianco, L., McKeen, S. A., Senff, C. J., Trainer, M., Tucker, S. C., and Zamora, R. J.: Evaluation of urban surface parameterizations in the WRF model using measurements during the Texas Air Quality Study 2006 field campaign, Atmos. Chem. Phys., 11, 2127–2143, doi:10.5194/acp-11-2127-2011, 2011.

Lapworth, A.: Factors determining the decrease in surface wind speed following the evening transition. Q.J.R. Meteorol. Soc., 129: 1945-1968. doi:10.1256/qj.02.163, 2003.

Li, M., Wang, T., Xie, M., Zhuang, B., Li, S., Han, Y. and Cheng, N.: Modeling of urban heat island and its impacts on thermal circulations in the Beijing-Tianjin-Hebei region, China. Theor. App. Clim., 128, 999-1013, 2017.

Li, Y., Barth, M. C. and Steiner, A. L.: Comparing turbulent mixing of atmospheric oxidants across model scales, Atmos. Environ., 199, 88–101, https://doi.org/10.1016/j.atmosenv.2018.11.004, 2019a.

Li, Y., Zhang, J., Sailor, D. J., and Ban-Weiss, G. A.: Effects of urbanization on regional meteorology and air quality in Southern California, Atmos. Chem. Phys., 19, 4439-4457, https://doi.org/10.5194/acp-19-4439-2019, 2019b.

Liao, J., Wang, T., Wang, X., Xie, M., Jiang, Z., Huang, X. and Zhu, J.: Impacts of different urban canopy schemes in WRF/Chem on regional climate and air quality in Yangtze River Delta, China, Atmos. Res., 145–146, 226–243, https://doi.org/10.1016/j.atmosres.2014.04.005, 2014.

Louis, J. F.: A Parametric Model of Vertical Eddy Fluxes in the Atmosphere, Bound. Lay. Meteor., 17, 187-202, 1979.

Markakis, K., Valari, M., Perrussel, O., Sanchez, O., and Honore, C.: Climate-forced air-quality modeling at the urban scale: sensitivity to model resolution, emissions and meteorology, Atmos. Chem. Phys., 15, 7703–7723, doi:10.5194/acp-15-7703-2015, 2015.

Masson, V., Gomes, L., Pigeon, G., Liousse, C., Pont, V., Lagouarde, J.-P., Voogt, J., Salmond, J., Oke, T. R., Hidalgo, J., Legain, D., Garrouste, O., Lac, C., Connan, O., Briottet, X., Lachérade, S., and Tulet, P.: The Canopy and Aerosol Particles Interactions in TOulouse Urban Layer (CAPITOUL) experiment, Meteorol. Atmos. Phys., 102, 135, https://doi.org/10.1007/s00703-008-0289-4, 2008.

Martilli, A., Yves-Alain Roulet, Martin Junier, Frank Kirchner, Mathias W. Rotach, Alain Clappier, On the impact of urban surface exchange parameterisations on air quality simulations: the Athens case, Atmospheric Environment, Volume 37, Issue 30, September 2003, Pages 4217-4231, ISSN 1352-2310, http://dx.doi.org/10.1016/S1352-2310(03)00564-8, 2003.

Mellor, G. and Yamada, T.: Development of a turbulence closure model for geophysical fluid problems, Rev. Astrophys. Space Phys., 20, 851-875, 1982.

Myhre, G., Grini, A., and Metzger, S.: Modelling of nitrate and ammonium-containing aerosols in presence of sea salt, Atmos. Chem. Phys., 6, 4809-4821, doi:10.5194/acp-6-4809-2006, 2006.

Nenes, A., Pandis, S. N., and Pilinis, C.: ISORROPIA: a new thermodynamic equilibrium model for multiphase multicomponent inorganic aerosols, Aquat. Geochem., 4, 123–152, 1998.

https://doi.org/10.5194/acp-2019-486
Preprint. Discussion started: 26 June 2019


Atmospheric Chemistry and Physics Discussions

Nogherotto, R., Tompkins, A. M., Giuliani, G., Coppola, E., and Giorgi, F.: Numerical framework and performance of the new multiple-phase cloud microphysics scheme in RegCM4.5: precipitation, cloud microphysics, and cloud radiative effects, Geosci. Model Dev., 9, 2533-2547, https://doi.org/10.5194/gmd-9-2533-2016, 2016.

O'Brien, J. J.: A note on the vertical structure of the eddy exchange coefficient in the planetary boundary layer, J. Atmos. Sci., 27, 1213–1215, 1970.

Oke, T. R.: The energetic basis of the urban heat island, Q. J. Roy. Meteor. Soc., 108, 1–24, https://doi.org/10.1002/qj.49710845502, 1982.

Oke, T., Mills, G., Christen, A., and Voogt, J.: Urban Climates, Cambridge University Press, https://doi.org/10.1017/9781139016476, 2017.

Oleson, K. W., Bonan, G. B., Feddema, J., Vertenstein, M., and Grimmond, C. S. B.: An urban parameterization for a global climate model. 1. Formulation and evaluation for two cities. J. Appl. Meteor. Clim., 47,1038–1060, 2008.

Oleson, K.W., Bonan, G.B., Feddema, J. and Vertenstein, M.: An urban parameterization for a global climate model. 2. Sensitivity to input parameters and the simulated urban heat island in offline simulations, J. Appl. Meteor. Clim., 47, 1061–1076, 2008.

Oleson, K., Lawrence, D. M., Bonan, G. B., Drewniak, B., Huang, M., Koven, C. D., Levis, S., Li, F., Riley, W. J., Subin, Z. M., Swenson, S. C., Thornton, P. E., Bozbiyik, A., Fisher, R., Heald, C. L., Kluzek, E., Lamarque, J.-F., Lawrence, P. J., Leung, L. R., Lipscomb, W., Muszala, S., Ricciuto, D. M., Sacks, W., Sun, Y., Tang, J., and Yang, Z.-L.: Technical Description of version 4.5 of the Community Land Model (CLM), NCAR Technical Note NCAR/TN-503+STR, Boulder, Colorado, 420 pp., 2013.

Pal, J. S., Small, E. E., and Eltahir, E. A. B.: Simulation of regional scale water and energy budgets: representation of subgrid cloud and precipitation processes within RegCM, J. Geophys. Res.-Atmos., 105, 29579–29594, 2000.

Pal, S., Xueref-Remy, I., Ammoura, L., Chazette, P., Gibert, F., Royer, P., Dieudonné, E., Dupont, J. C.. Haeffelin, M., Lac, C., Lopez, M., Morille, Y. and Ravetta, F.: Spatio-temporal variability of the atmospheric boundary layer depth over the Paris agglomeration: An assessment of the impact of the urban heat island intensity, Atmos. Environ., 261-275, https://doi.org/10.1016/j.atmosenv.2012.09.046, 2012.

Passant, N.: Speciation of UK Emissions of Non-methane Volatile Organic Compounds, DEFRA, Oxon, UK, 2002.

de la Paz, D., Borge, R. and Martilli, A.: Assessment of a high resolution annual WRF-BEP/CMAQ simulation for the urban area of Madrid (Spain), Atmos. Environ., 144, 282–296, 2016.

Pichierri, M., Bonafoni, S., and Biondi, R.: Satellite air temperature estimation for monitoring the canopy layer heat island of Milan, Remote Sens. Environ., 127, 130–138, https://doi.org/10.1016/j.rse.2012.08.025, 2012.

Pleim, J.E.: A Combined Local and Nonlocal Closure Model for the Atmospheric Boundary Layer. Part I: Model Description and Testing, J. Appl. Meteor. Climatol., 46, 1383-1395, https://doi.org/10.1175/JAM2539.1, 2007.

Ren, Y., Zhang, H., Wei, W., Wu, B., Cai, X., and Song, Y.: Effects of turbulence structure and urbanization on the heavy haze pollution process, Atmos. Chem. Phys., 19, 1041-1057, https://doi.org/10.5194/acp-19-1041-2019, 2019.

Richards, K.: Observation and simulation of dew in rural and urban environments, Prog. Phys. Geog., 28, 76–94, 2004.

Roth, M.: Review of atmospheric turbulence over cities, Q. J. Roy. Meteor. Soc., 126, 941–990, 2000.

Ryu, Y.-H., Baik, J.-J., Kwak, K.-H., Kim, S., and Moon, N.: Impacts of urban land-surface forcing on ozone air quality in the Seoul metropolitan area, Atmos. Chem. Phys., 13, 2177-2194, doi:10.5194/acp-13-2177-2013, 2013a.

Ryu, Y.-H., Baik, J.-J., and Lee, S.-H.: Effects of anthropogenic heat on ozone air quality in a megacity, Atmos. Environ., 80, 20–30, https://doi.org/10.1016/j.atmosenv.2013.07.053, 2013b.

Sarrat, C., Lemonsu, A., Masson, V., and Guedalia, D.: Impact of urban heat island on regional atmospheric pollution, Atmos. Environ., 40, 1743–1758, 2006.

https://doi.org/10.5194/acp-2019-486
Preprint. Discussion started: 26 June 2019




Schaap, M., van Loon, M., ten Brink, H. M., Dentener, F. J., and Builtjes, P. J. H.: Secondary inorganic aerosol simulations for Europe with special attention to nitrate, Atmos. Chem. Phys., 4, 857-874, doi:10.5194/acp-4-857-2004, 2004.

Seinfeld, J. H. and Pandis, S. N.: Atmospheric Chemistry and Physics: From Air Pollution to Climate Change, J. Wiley, New York, 1998.

Simmons, A. J., Willett, K. M., Jones, P. D., Thorne, P. W., and Dee, D. P.: Low-frequency variations in surface atmospheric humidity, temperature and precipitation: inferences from reanalyses and monthly gridded observational datasets, J. Geophys. Res., 115, D01110, doi:10.1029/2009JD012442, 2010.

Stock, Z. S., Russo, M. R., Butler, T. M., Archibald, A. T., Lawrence, M. G., Telford, P. J., Abraham, N. L., and Pyle, J. A.: Modelling the impact of megacities on local, regional and global tropospheric ozone and the deposition of nitrogen species, Atmos. Chem. Phys., 13, 12215–12231, doi:10.5194/acp-13-12215-2013, 2013.

Strader, R. Lurmann, F. and Pandis, S. N.: Evaluation of secondary organic aerosol formation in winter, Atmos. Environ., 33., 4849-4863, 1999.

Struzewska, J. and Kaminski, J. W.: Impact of urban parameterization on high resolution air quality forecast with the GEM – AQ model, Atmos. Chem. Phys., 12, 10387–10404, https://doi.org/10.5194/acp-12-10387-2012, 2012.

Stutz, J., Alicke, B., Ackermann, R., Geyer, A., White, A., and Williams, E.: Vertical profiles of NO3, N2O5, O3, and NOx in the nocturnal boundary layer: 1. Observations during the Texas Air Quality Study 2000, J. Geophys. Res., 109, D12 306, doi:10.1029/2003JD004209, 2004.

Tao, Z., Santanello, J. A., Chin, M., Zhou, S., Tan, Q., Kemp, E. M., and Peters-Lidard, C. D.: Effect of land cover on atmospheric processes and air quality over the continental United States – a NASA Unified WRF (NU-WRF) model study, Atmos. Chem. Phys., 13, 6207-6226, doi:10.5194/acp-13-6207-2013, 2013.

Tie, X., Brasseur, G., and Ying, Z.: Impact of model resolution on chemical ozone formation in Mexico City: application of the WRF-Chem model, Atmos. Chem. Phys., 10, 8983-8995, https://doi.org/10.5194/acp-10-8983-2010, 2010.

Tiedtke, M.: A Comprehensive Mass Flux Scheme for Cumulus Parameterization in Large-Scale Models, Mon. Weather Rev., 117, 1779-1800, https://doi.org/10.1175/1520-0493(1989)117, 1989.

Varentsov, M., Konstantinov, P., Baklanov, A., Esau, I., Miles, V., and Davy, R.: Anthropogenic and natural drivers of a strong winter urban heat island in a typical Arctic city, Atmos. Chem. Phys., 18, 17573-17587, https://doi.org/10.5194/acp-18-17573-2018, 2018.

Wang, X. M., Lin, W. S., Yang, L. M., Deng, R. R., and Lin, H.: A numerical study of influences of urban land-use change on ozone distribution over the Pearl River Delta region, China, Tellus, 59B, 633–641, 2007.

Wang, X., Chen, F., Wu, Z., Zhang, M., Tewari, M., Guenther, A., and Wiedinmyer, C.: Impacts of weather conditions modified by urban expansion on surface ozone: Comparison between the Pearl River Delta and Yangtze River Delta regions, Adv. Atmos. Sci., 26, 962–972, 2009.

Wang, J., Feng, J., Yan, Z., Hu, Y., and Jia, G.: Nested high-resolution modeling of the impact of urbanization on regional climate in three vast urban agglomerations in China, J. Geophys. Res., 117, D21103, https://doi.org/10.1029/2012JD018226, 2012.

Wei, W., Zhang, H., Wu, B., Huang, Y., Cai, X., Song, Y., and Li, J.: Intermittent turbulence contributes to vertical dispersion of PM2.5 in the North China Plain: cases from Tianjin, Atmos. Chem. Phys., 18, 12953-12967, https://doi.org/10.5194/acp-18-12953-2018, 2018.

Wong, K. W. and Stutz, J.: Influence of nocturnal vertical stability on daytime chemistry: a one-dimensional model study, Atmos. Environ., 44, 3753–3760, https://doi.org/10.1016/j.atmosenv.2010.06.057, 2010.

https://doi.org/10.5194/acp-2019-486
Preprint. Discussion started: 26 June 2019


Atmospheric Chemistry and Physics Discussions

Xie, M., Zhu, K., Wang, T., Feng, W., Gao, D., Li, M., Li, S., Zhuang, B., Han, Y., Chen, P., and Liao, J.: Changes in regional meteorology induced by anthropogenic heat and their impacts on air quality in South China, Atmos. Chem. Phys., 16, 15011-15031, doi:10.5194/acp-16-15011-2016, 2016a.

Xie, M., Liao, J. B., Wang, T. J., Zhu, K. G., Zhuang, B. L., Han, Y., Li, M. M. and Li, S.: Modeling of the anthropogenic heat flux and its effect on regional meteorology and air quality over the Yangtze River Delta region, China, Atmos. Chem. Phys., 16, 6071-6089, doi:10.5194/acp-16-6071-2016, 2016b.

Yarwood. G., Rao, S., Yocke, M., and Whitten, G. Z.: Updates to the Carbon Bond chemical mechanism: CB05, Final Report prepared for US EPA, http://www.camx.com/publ/pdfs/CB05_Final_Report_120805.pdf, Novato, NC, USA, 2005.

Žák, M., Nita, A., Dumitrescu, A., Sorin, Ch.: Influence of synoptic scale atmospheric circulation on the development of urban heat island in Prague and Bucharest, Urban Climate, in review, 2019.

Zanis, P., Katragkou, E., Tegoulias, I., Poupkou, A., Melas, D., Huszar, P. and Giorgi, F.: Evaluation of near surface ozone in air quality simulations forced by a regional climate model over Europe for the period 1991–2000, Atmos. Environ., 45, 6489–6500, https://doi.org/10.1016/j.atmosenv.2011.09.001, 2011.

Zha, J., Zhao, D., Wu, J. and Zhang, P.: Numerical simulation of the effects of land use and cover change on the near-surface wind speed over Eastern China, Clim. Dyn., https://doi.org/10.1007/s00382-019-04737-w, 2019.

Zhang, L., Brook, J. R., and Vet, R.: A revised parameterization for gaseous dry deposition in air-quality models, Atmos. Chem. Phys., 3, 2067-2082, https://doi.org/10.5194/acp-3-2067-2003, 2003.

Zhang, D., and Zheng, W.: Diurnal Cycles of Surface Winds and Temperatures as Simulated by Five Boundary Layer Parameterizations. J. Appl. Meteor., 43, 157–169, doi:10.1175/1520-0450(2004)043, 2004.

Zhao, L., Lee, X., and Schultz, N. M.: A wedge strategy for mitigation of urban warming in future climate scenarios, Atmos. Chem. Phys., 17, 9067-9080, https://doi.org/10.5194/acp-17-9067-2017, 2017.

Zhong, S., Qian, Y., Zhao, C., Leung, R., Wang, H., Yang, B., Fan, J., Yan, H., Yang, X.-Q., and Liu, D.: Urbanization-induced urban heat island and aerosol effects on climate extremes in the Yangtze River Delta region of China, Atmos. Chem. Phys., 17, 5439-5457, https://doi.org/10.5194/acp-17-5439-2017, 2017.

Zhong, S., Qian, Y., Sarangi, C., Zhao, C., Leung, R., Wang, H., et al.: Urbanization effect on winter haze in the Yangtze River Delta region of China, Geophys. Res. Letters, 45., https://doi.org/10.1029/2018GL077239, 2018.

Zhu, B., Kang, H., Zhu, T., Su, J., Hou, X., and Gao, J. Impact of Shanghai urban land surface forcing on downstream city ozone chemistry, J. Geophys. Res., 120(9) 4340-4351, 2015.

Zhu, K., Xie, M., Wang, T., Cai, J., Li, S., and Feng, W.: A modeling study on the effect of urban land surface forcing to regional meteorology and air quality over South China, Atmos. Environ., 152, 389–404, http://dx.doi.org/10.1016/j.atmosenv.2016.12.053, 2017.

https://doi.org/10.5194/acp-2019-486
Preprint. Discussion started: 26 June 2019


Atmospheric Chemistry and Physics Discussions

**Table 1.** Model experiments (simulations) performed for RegCM (1st column) and for CAMx (other columns). The 2nd column denotes which urban effects are considered: NOURBAN – none; URB_t+q+uv – effect of temperature, humidity, wind; URB_t+q+uv+kv – effect of temperature, humidity, wind and trubulence. The 3rd column lists the $Kv$-methods used.

| Models | | | Domains | | |
|---|---|---|---|---|---|
| RegCM | CAMx | $Kv$-method | PHA27 | PHA09 | PHA03 |
| NOURBAN | NOURBAN | CMAQ | * | * | * |
| URBAN | URB_t+q+uv | CMAQ | * | * | * |
| | | DIRECT | * | * | * |
| | | ACM2 | * | * | * |
| | | OB70 | * | * | * |
| | | MYJ | * | * | * |
| | | YSU | * | * | * |
| | URB_t+q+uv+kv | CMAQ | * | * | * |
| | | DIRECT | * | * | * |
| | | ACM2 | * | * | * |
| | | OB70 | * | * | * |
| | | MYJ | * | * | * |
| | | YSU | * | * | * |

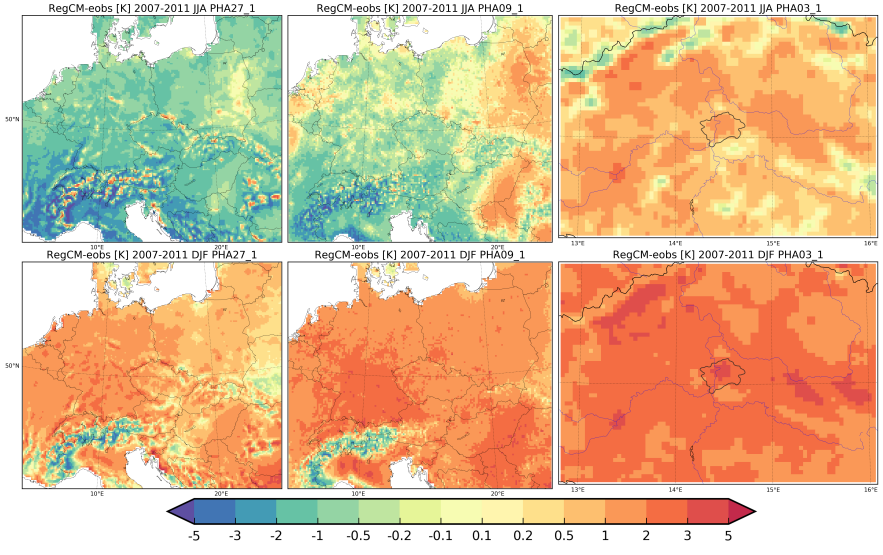


**Figure 1.** The difference between RegCM model near surface temperature and E-OBS data for 2007-2011 JJA (upper row) and DJF (lower row) for the 27, 9 and 3 km domain (columns) in ° C. Note that the 27 km domain is cropped to show only the part corresponding to the 9 km domain. For the right panel, the administrative boundary of Prague is indicated too.

https://doi.org/10.5194/acp-2019-486
Preprint. Discussion started: 26 June 2019


Atmospheric Chemistry and Physics Discussions

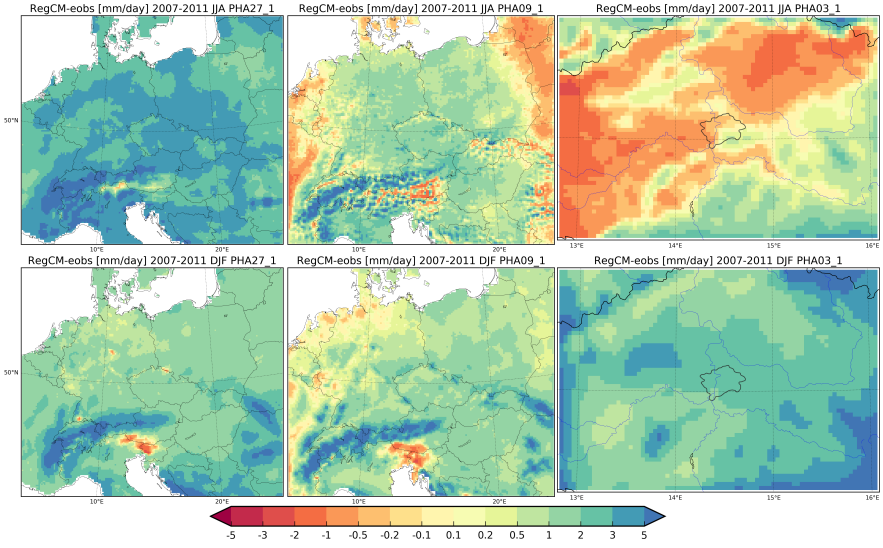


**Figure 2.** The difference between RegCM model precipitation and E-OBS data for 2007-2011 JJA (upper row) and DJF (lower row) for the 27, 9 and 3 km domain (columns) in $\mathrm{mmday}^{-1}$. Note that the 27 km domain is cropped to show only the part corresponding to the 9 km domain. For the right panel, the administrative boundary of Prague is indicated too.

https://doi.org/10.5194/acp-2019-486
Preprint. Discussion started: 26 June 2019


Atmospheric Chemistry and Physics Discussions

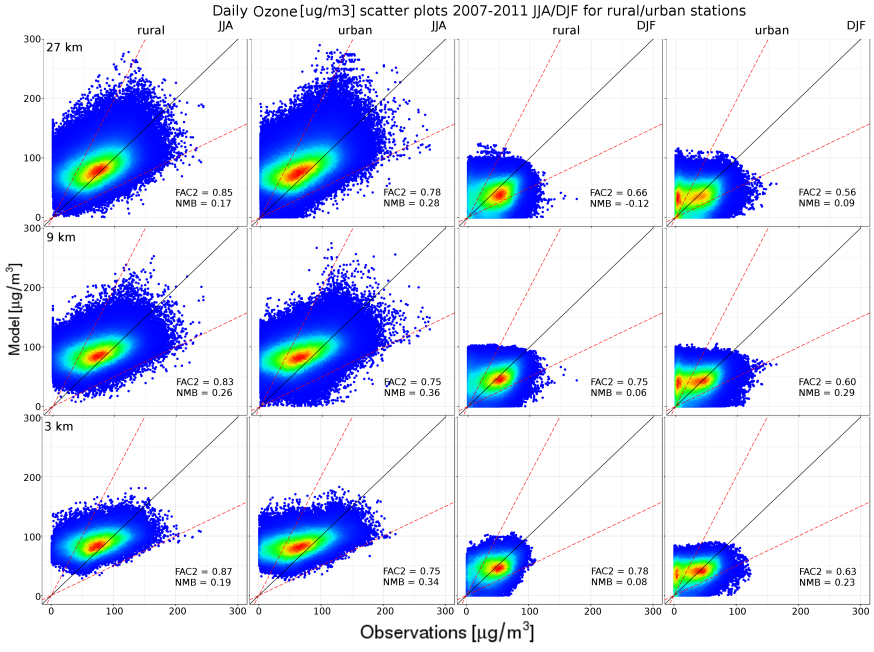


**Figure 3.** Scatter plots of daily ozone values for JJA (1st and 2nd column) and DJF (3rd and 4th column) for rural and urban stations in $\mu g m^{-3}$. The rows represent different model resolutions from 27 km (top) to 3 km (bottom). Dot colors stand for the density of the model-observation pairs. Red dashed lines define the ”factor-2“ (FAC2) region. Calculated values of FAC2 and the normalized mean bias (NMB) are indicated too.

https://doi.org/10.5194/acp-2019-486
Preprint. Discussion started: 26 June 2019


Atmospheric Chemistry and Physics Discussions

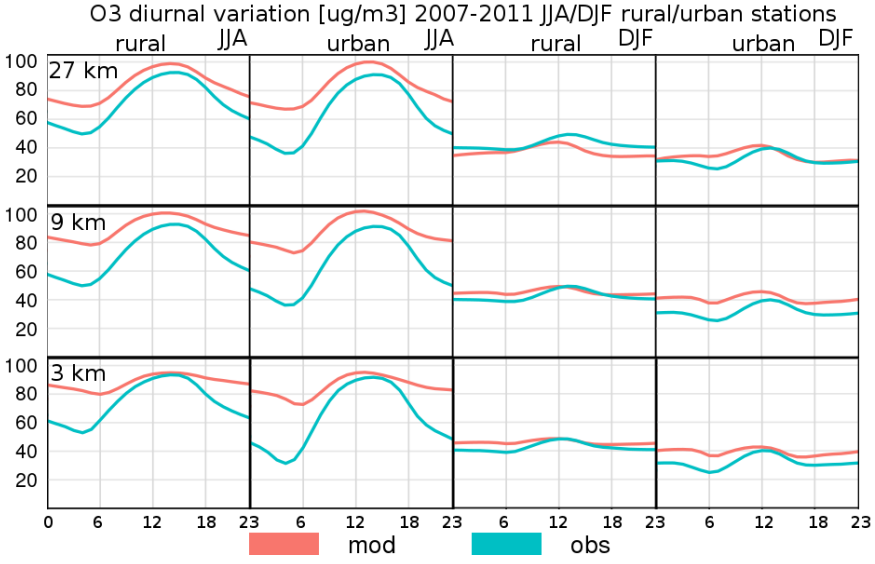


**Figure 4.** Comparison of average diurnal cycles of ozone with measurements $\mu g m^{-3}$ for JJA (1st and 2nd columns) and DJF (3rd and 4th columns) for rural and urban background stations for the three domains (27 km, 9 km and 3 km, from top to bottom): model (red), observation (green).

https://doi.org/10.5194/acp-2019-486
Preprint. Discussion started: 26 June 2019


Atmospheric Chemistry and Physics Discussions

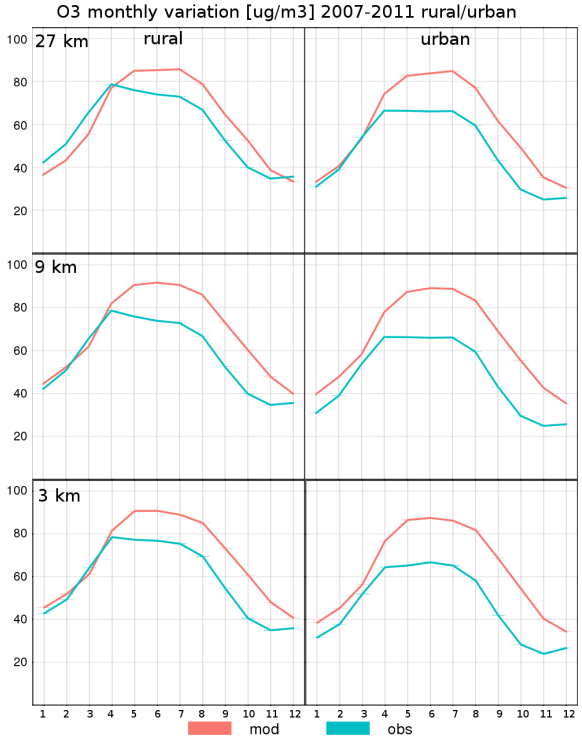


**Figure 5.** Comparison of monthly ozone values with measurements daily in $\mu gm^{-3}$ for rural (left) and urban background stations (right) for the three domains (27 km, 9 km and 3 km, from top to bottom): model (red), observation (green).

https://doi.org/10.5194/acp-2019-486
Preprint. Discussion started: 26 June 2019


Atmospheric Chemistry and Physics Discussions

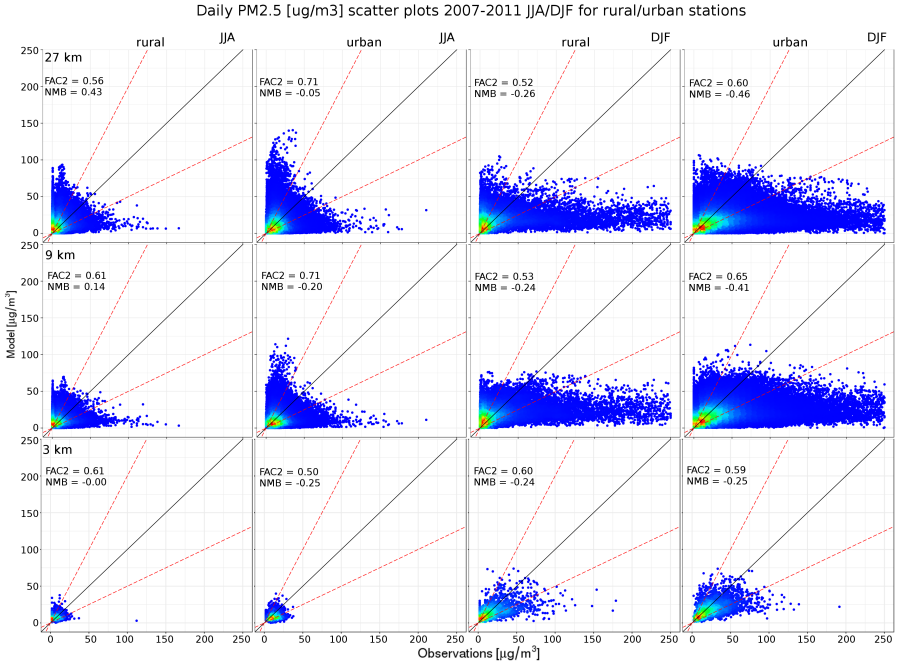


**Figure 6.** Scatter plots of daily PM2.5 values for JJA (1st and 2nd column) and DJF (3rd and 4th column) for rural and urban stations in $\mu g m^{-3}$. The rows represent different model resolutions from 27 km (top) to 3 km (bottom). Dot colors stand for the density of the model-observation pairs. Red dashed lines define the "factor-2" (FAC2) region. Calculated values of FAC2 and the normalized mean bias (NMB) are indicated too.

https://doi.org/10.5194/acp-2019-486
Preprint. Discussion started: 26 June 2019


Atmospheric Chemistry and Physics Discussions

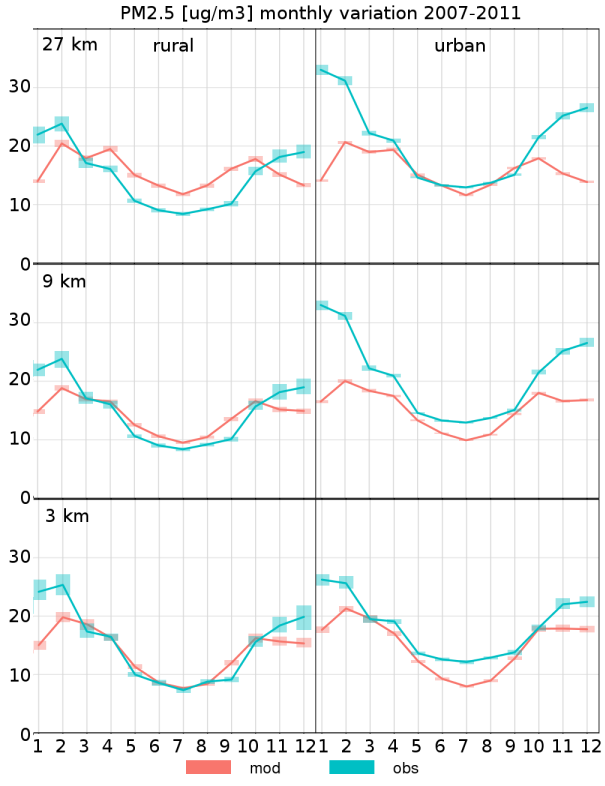


**Figure 7.** Comparison of monthly PM2.5 concentrations with measurements daily in $\mu g m^{-3}$ for rural (left) and urban background stations (right) for the three domains (27 km, 9 km and 3 km, from top to bottom): model (red), observation (green).

https://doi.org/10.5194/acp-2019-486
Preprint. Discussion started: 26 June 2019


Atmospheric Chemistry and Physics Discussions

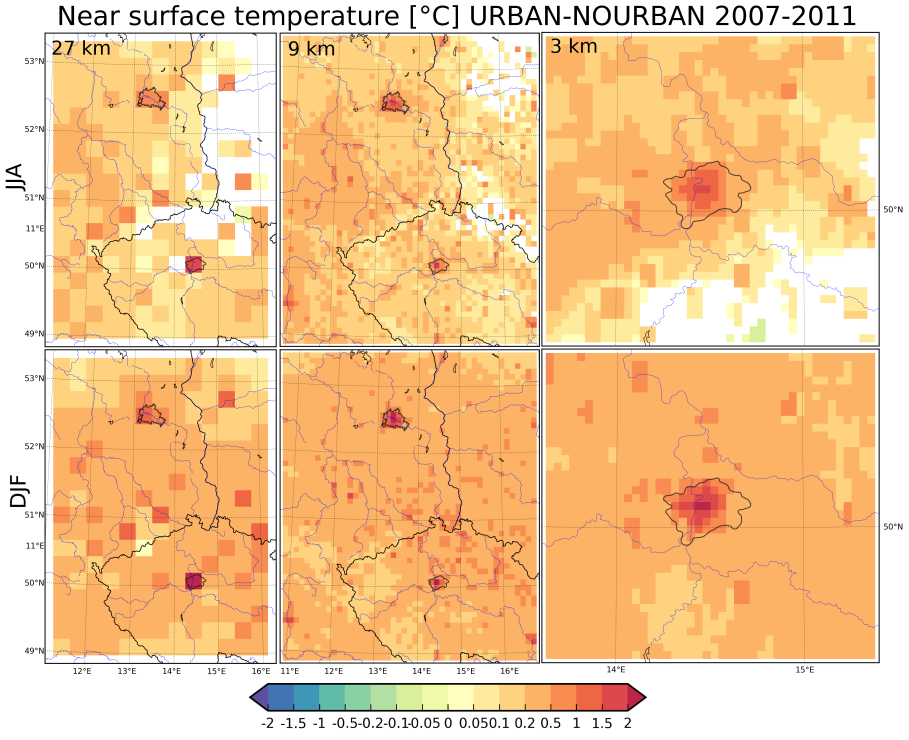


**Figure 8.** Impact of urban surfaces on near surface temperature in °C for JJA (upper) and DJF (lower row) for the three resolutions (27, 9 and 3 km). Shaded areas represent statistically significant changes over the 98% threshold using two tailed t-test. The geographic location of Berlin and Prague is indicated by their administrative boundary.

https://doi.org/10.5194/acp-2019-486
Preprint. Discussion started: 26 June 2019


Atmospheric Chemistry and Physics Discussions

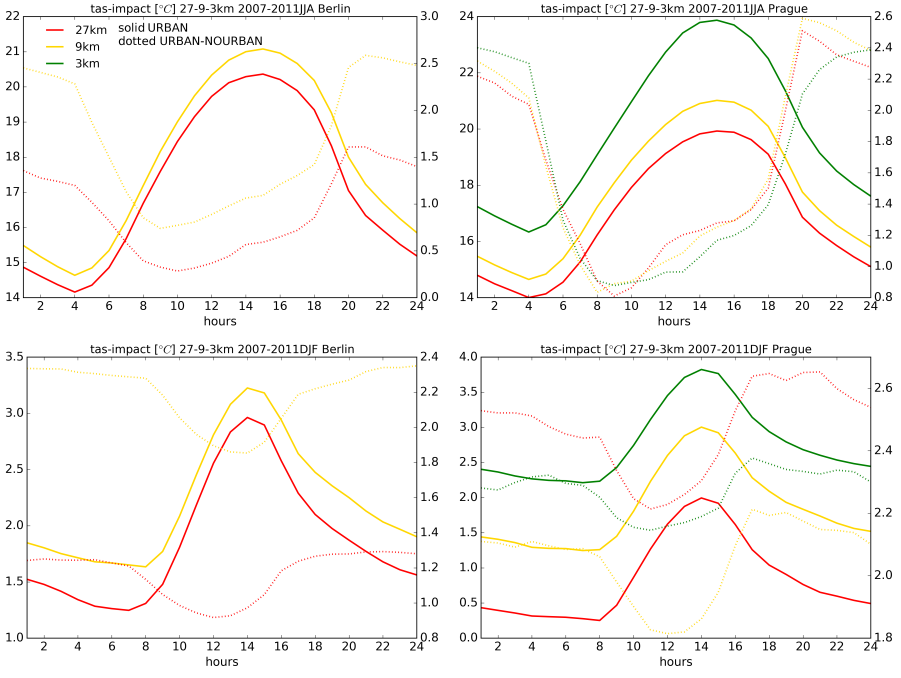


**Figure 9.** Impact of urban surfaces on near surface temperature diurnal cycle in °C for JJA (upper) and DJF (lower row) for the three resolutions (27 km – red, 9 km – orange and 3 km – dark green). Solid lines are the absolute values from the URBAN model experiment, dashed lines represent the urban impact.

https://doi.org/10.5194/acp-2019-486
Preprint. Discussion started: 26 June 2019


Atmospheric Chemistry and Physics Discussions

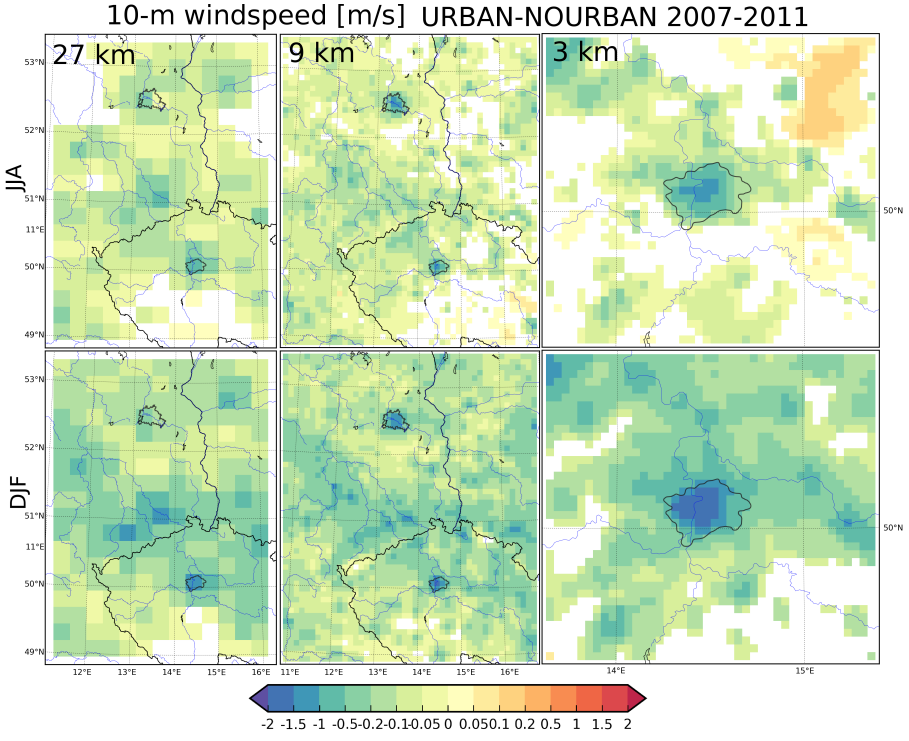


**Figure 10.** Impact of urban surfaces on 10 m wind speed in $\mathrm{ms}^{-1}$ for JJA (upper) and DJF (lower row) for the three resolutions (27, 9 and 3 km). Shaded areas represent statistically significant changes over the 98% threshold using two tailed t-test. The geographic location of Berlin and Prague is indicated by their administrative boundary.

https://doi.org/10.5194/acp-2019-486
Preprint. Discussion started: 26 June 2019


Atmospheric Chemistry and Physics Discussions

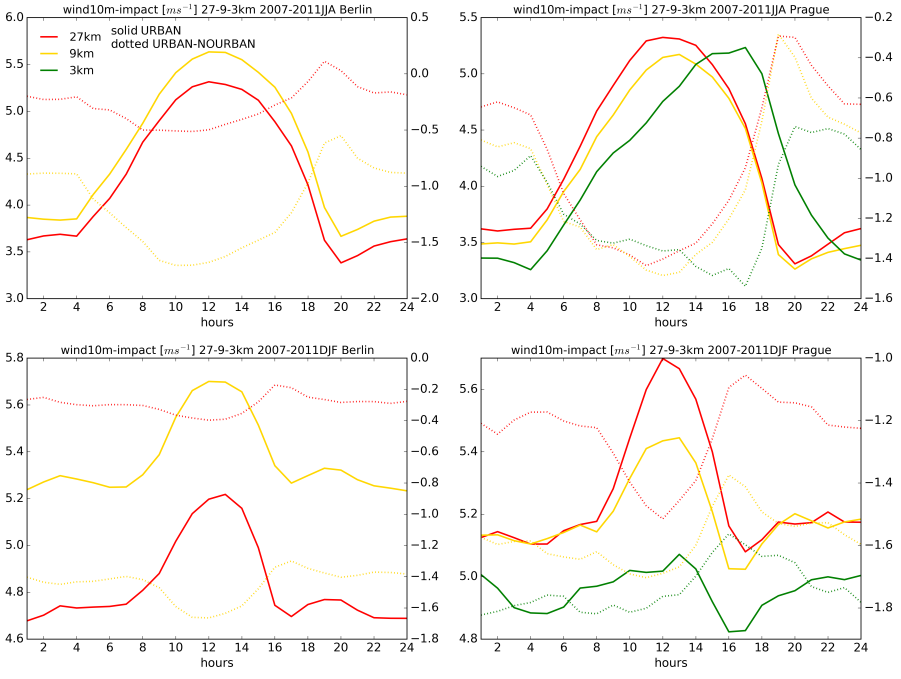


**Figure 11.** Impact of urban surfaces on the diurnal cycle of the 10 m wind speed in $\mathrm{ms}^{-1}$ for JJA (upper) and DJF (lower row) for the three resolutions (27 km – red, 9 km – orange and 3 km – dark green). Solid lines are the absolute values from the URBAN model experiment, dashed lines represent the urban impact.

https://doi.org/10.5194/acp-2019-486
Preprint. Discussion started: 26 June 2019


Atmospheric Chemistry and Physics Discussions

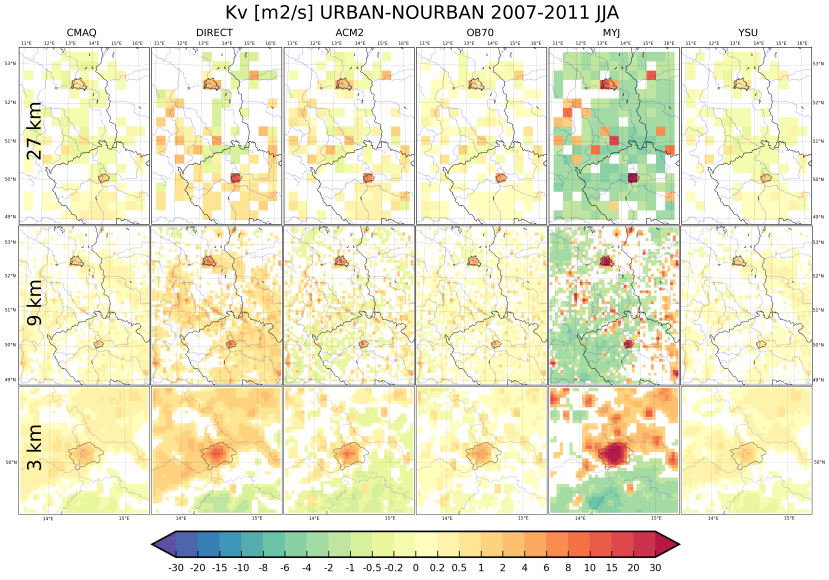


**Figure 12.** Impact of urban surfaces on the vertical eddy diffusion coefficient at 65 m in $m^2 s^{-1}$ for the 27 km (upper), 9 km (middle) and 3 km (lower row) for each $Kv$ methods (CMAQ, DIRECT, ACM2, OB70, MYJ and YSU, from left to right). Shaded areas represent statistically significant changes over the 98% threshold using two tailed t-test. The geographic location of Berlin and Prague is indicated by their administrative boundary.

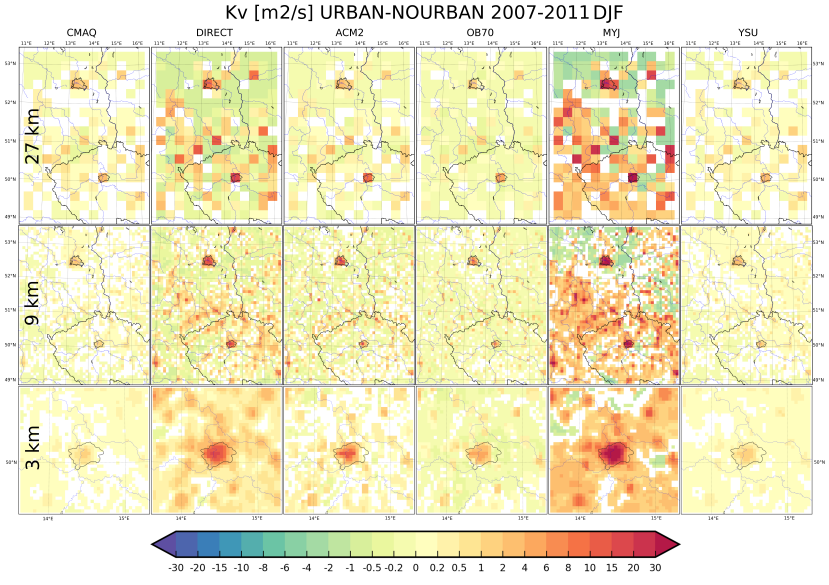


**Figure 13.** Same as Fig. 12 but for DJF.

https://doi.org/10.5194/acp-2019-486
Preprint. Discussion started: 26 June 2019


Atmospheric Chemistry and Physics Discussions

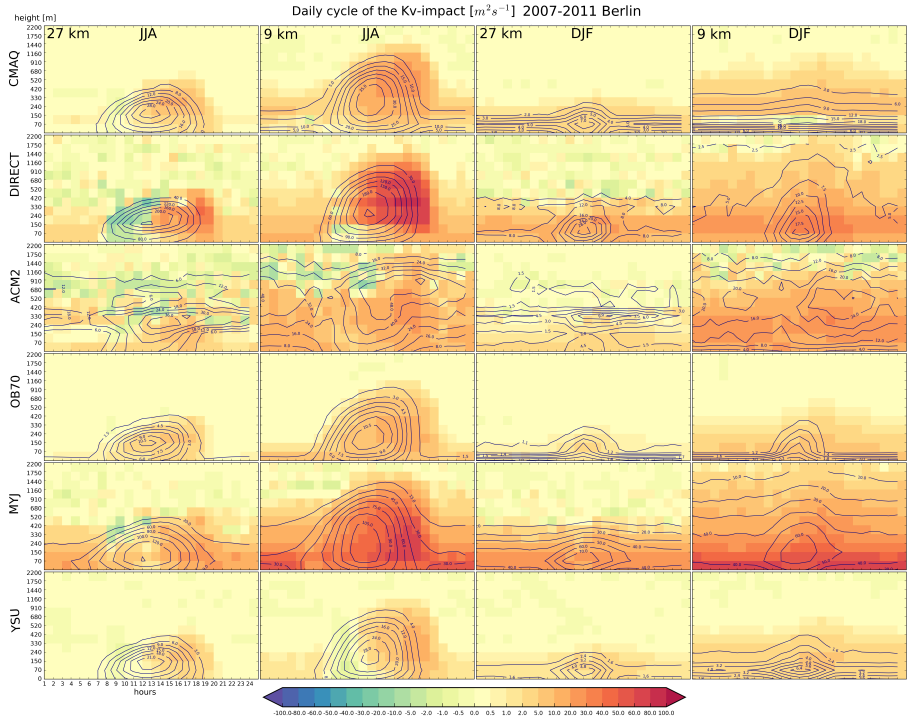


**Figure 14.** Impact of urban surfaces on the diurnal cycle of the vertical eddy diffusion profile in $\mathrm{m^2 s^{-1}}$ over Berlin for the 27 km (1st and 3rd column) and 9 km (2nd and 4th column) domains for both seasons (columns 1-2 JJA, columns 3-4 DJF). Individual rows represent different $Kv$ methods (CMAQ, DIRECT, ACM2, OB70, MYJ and YSU, from top to bottom). Contour lines denote the absolute $Kv$ values from the URBAN model experiment.

https://doi.org/10.5194/acp-2019-486
Preprint. Discussion started: 26 June 2019


Atmospheric Chemistry and Physics Discussions

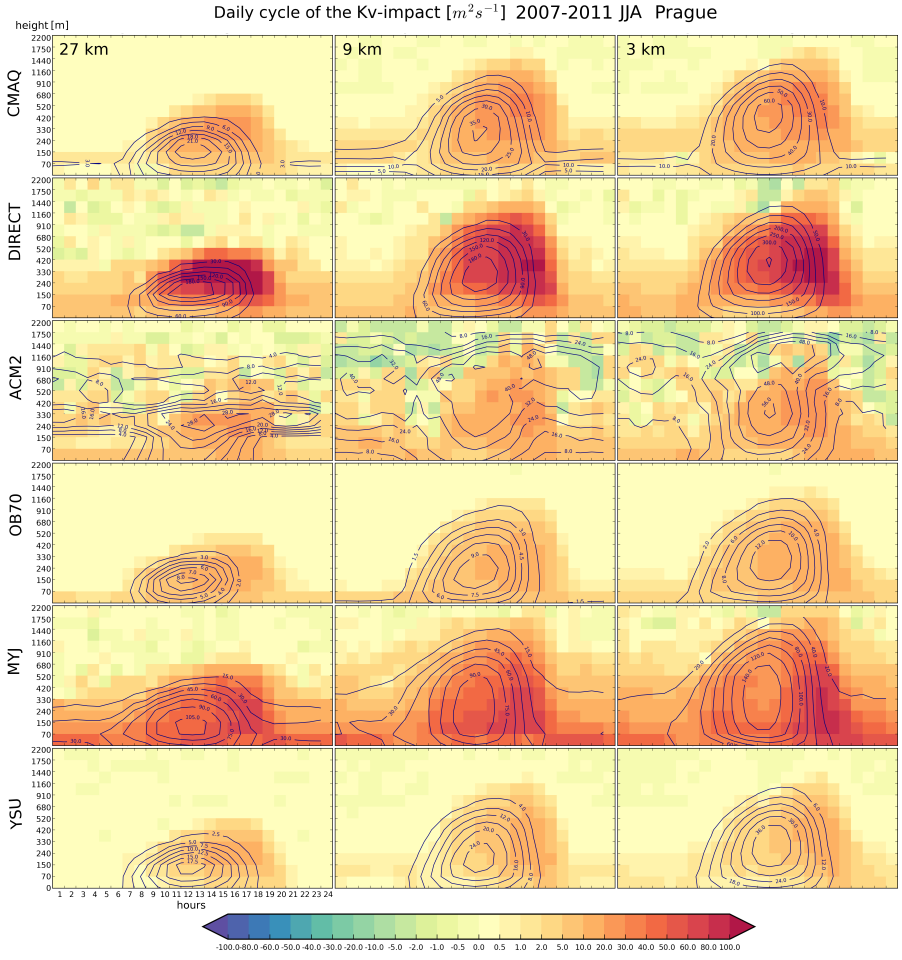


**Figure 15.** Impact of urban surfaces on the JJA diurnal cycle of the vertical eddy diffusion profile in $\mathrm{m^2 s^{-1}}$ over Prague for the 27, 9 and 3 km domains (columns from left to right)4th column) domains. Individual rows represent different $Kv$ methods (CMAQ, DIRECT, ACM2, OB70, MYJ and YSU, from top to bottom). Contour lines denote the absolute $Kv$ values from the URBAN model experiment.

https://doi.org/10.5194/acp-2019-486
Preprint. Discussion started: 26 June 2019


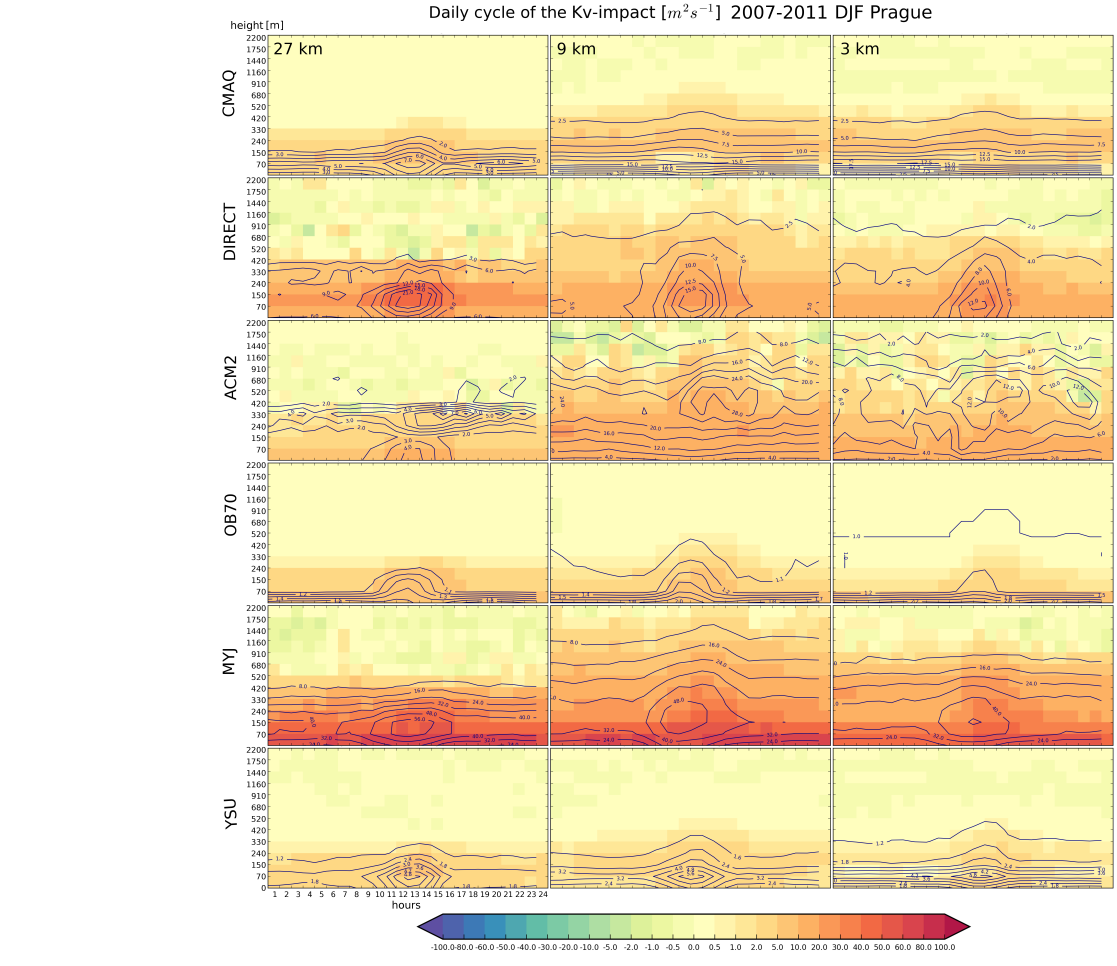


**Figure 16.** Impact of urban surfaces on the DJF diurnal cycle of the vertical eddy diffusion profile in $\mathrm{m^2 s^{-1}}$ over Prague for the 27, 9 and 3 km domains (columns from left to right)4th column) domains. Individual rows represent different $Kv$ methods (CMAQ, DIRECT, ACM2, OB70, MYJ and YSU, from top to bottom). Contour lines denote the absolute $Kv$ values from the URBAN model experiment.

https://doi.org/10.5194/acp-2019-486
Preprint. Discussion started: 26 June 2019


Atmospheric Chemistry and Physics Discussions

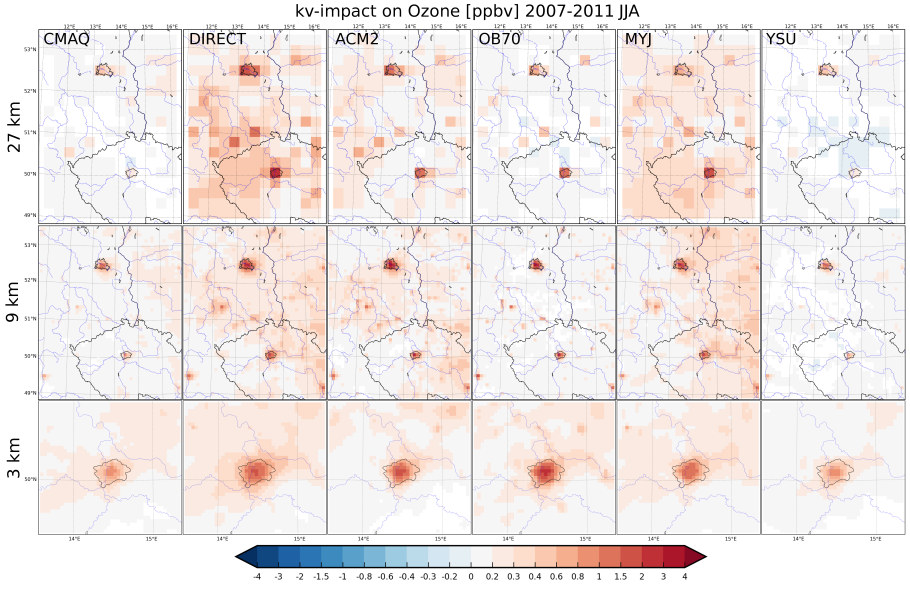


**Figure 17.** The impact of urbanization induced $Kv$ enhancement (i.e. increase of vertical eddy diffusivity) on surface $O_3$ concentrations in ppbv for the 27, 9 and 3 km resolutions (top to bottom) for JJA for the six $Kv$ methods (CMAQ, DIRECT, ACM2, OB70, MYJ and YSU). The geographic location of Berlin and Prague is indicated by their administrative boundary. Shaded areas represent statistically significant changes on the 98% level using two tailed t-test.

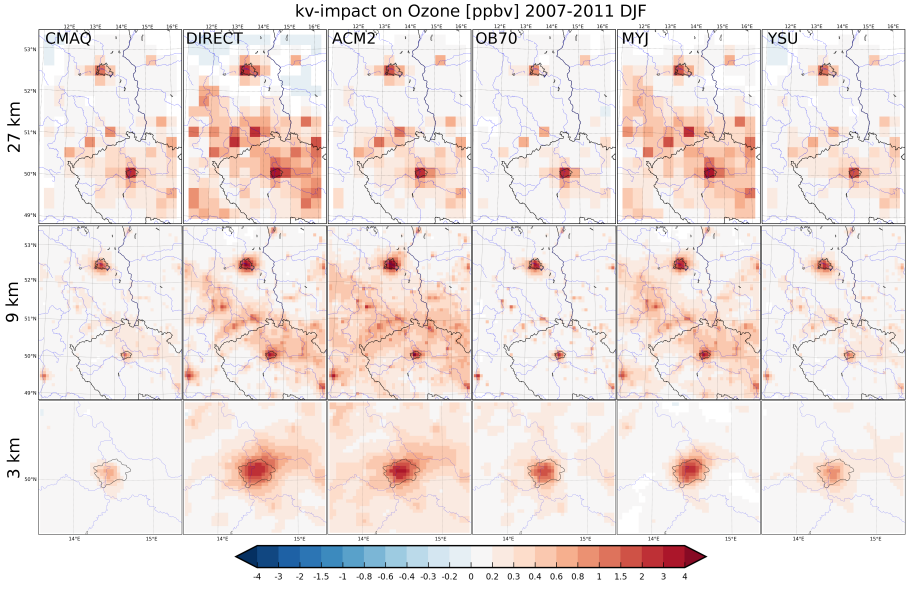


**Figure 18.** Same as Fig. 17 but for DJF.

https://doi.org/10.5194/acp-2019-486
Preprint. Discussion started: 26 June 2019


Atmospheric Chemistry and Physics Discussions

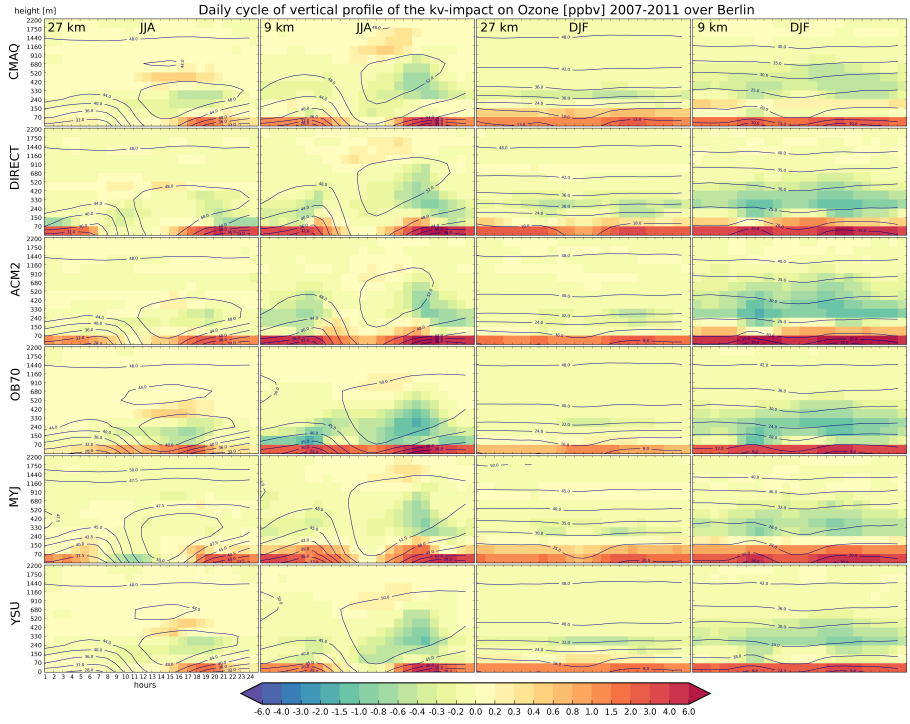


**Figure 19.** The impact of the urbanization induced $Kv$ enhancement (i.e. increase of vertical eddy diffusivity) on the diurnal cycle of the $O_3$ profile over Berlin for JJA (columns 1–2) and DJF (columns 3–4) evaluated over the 27 km (columns 1 and 3) and 9 km (columns 2 and 4) domains. Rows correspond to individual $Kv$-methods. Colors mean the difference, contours stand for the absolute concentrations (from the total-impact). Units in ppbv.

https://doi.org/10.5194/acp-2019-486
Preprint. Discussion started: 26 June 2019


Atmospheric Chemistry and Physics Discussions

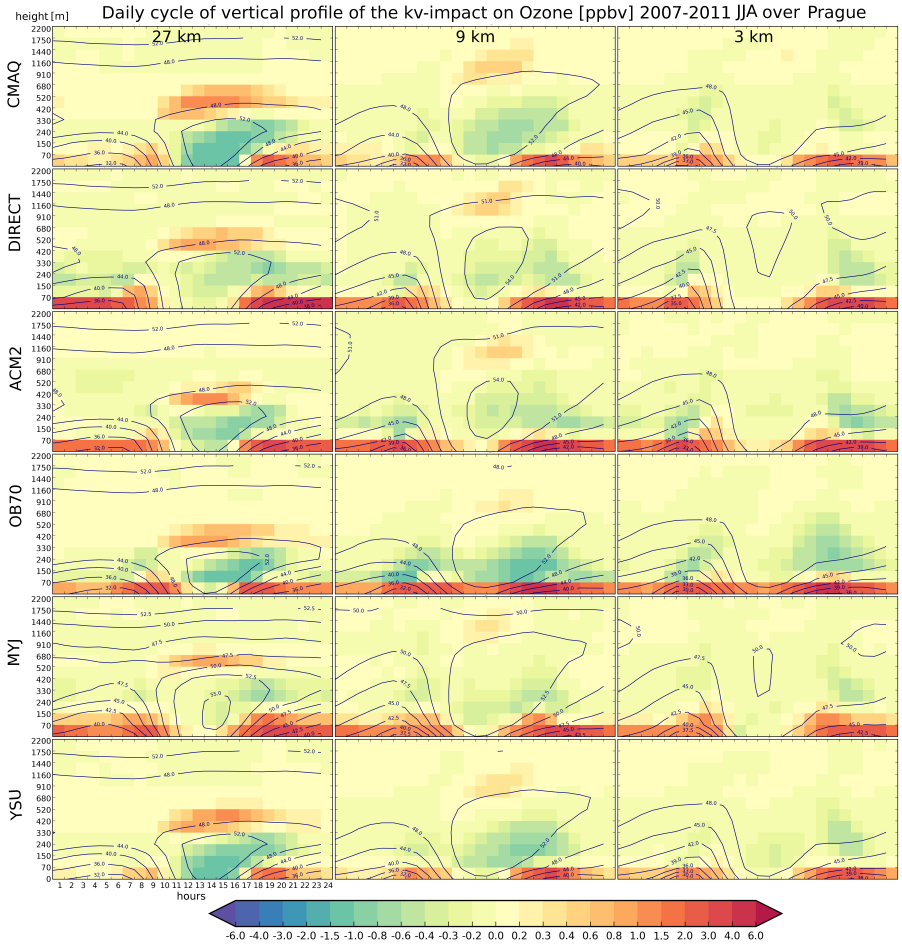


**Figure 20.** The impact of the urbanization induced $Kv$ enhancement (i.e. increase of vertical eddy diffusivity) on the diurnal cycle of the $O_3$ profile over Prague for JJA. Columns represent the three resolutions (27km, 9km and 3 km, from left to right). Rows correspond to individual $Kv$-methods. Colors mean the difference, contours stand for the absolute concentrations (from the total-impact). Units in ppbv.

https://doi.org/10.5194/acp-2019-486
Preprint. Discussion started: 26 June 2019


Atmospheric Chemistry and Physics Discussions

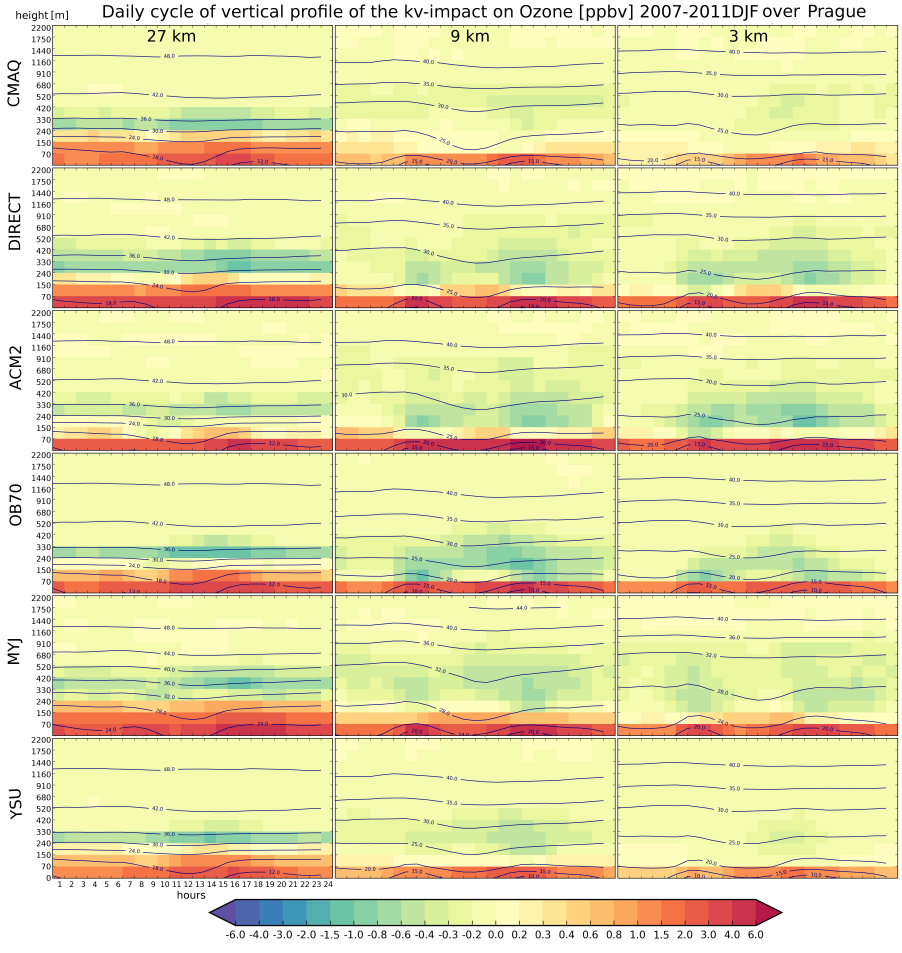


**Figure 21.** Same as Fig. 20 but for DJF.

https://doi.org/10.5194/acp-2019-486
Preprint. Discussion started: 26 June 2019


Atmospheric Chemistry and Physics Discussions

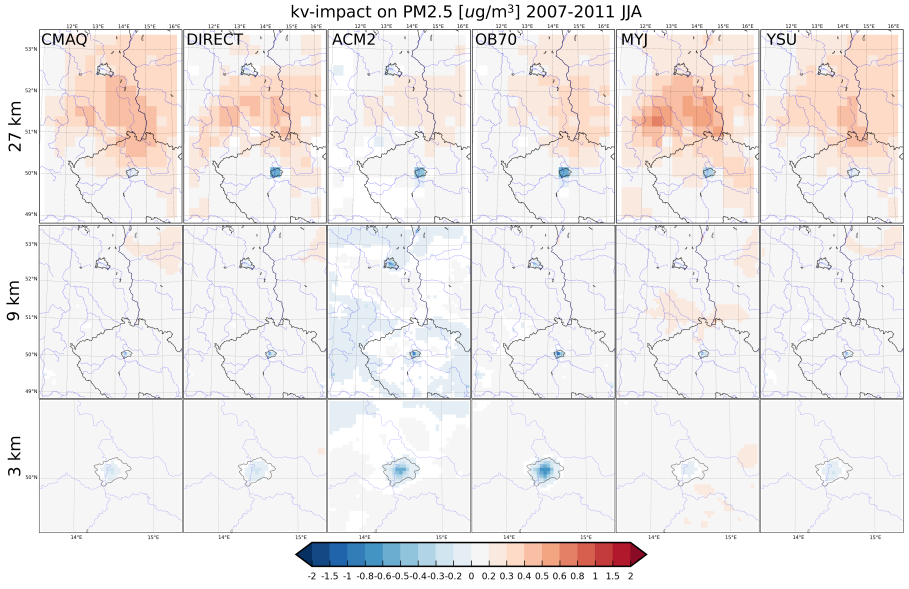


**Figure 22.** The impact of urbanization induced $Kv$ enhancement (i.e. increase of vertical eddy diffusivity) on surface $\mathrm{PM2.5}$ concentrations in $\mu\mathrm{gm}^{-3}$ for the 27, 9 and 3 km resolutions (top to bottom) for JJA for the six $Kv$ methods (CMAQ, DIRECT, ACM2, OB70, MYJ and YSU). The geographic location of Berlin and Prague is indicated by their administrative boundary. Shaded areas represent statistically significant changes on the 98% level using two tailed t-test.

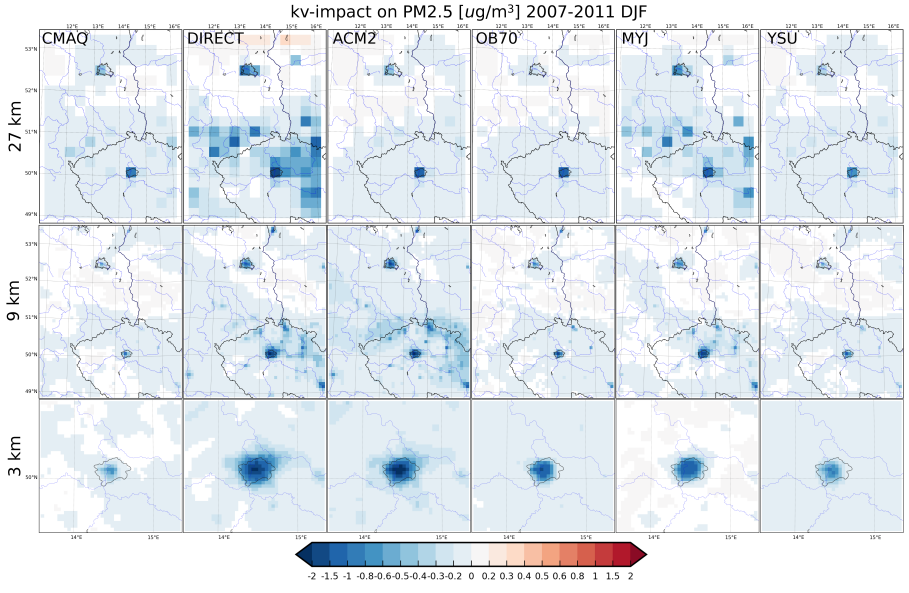


**Figure 23.** Same as Fig. 22 but for DJF.

https://doi.org/10.5194/acp-2019-486
Preprint. Discussion started: 26 June 2019


Atmospheric Chemistry and Physics Discussions

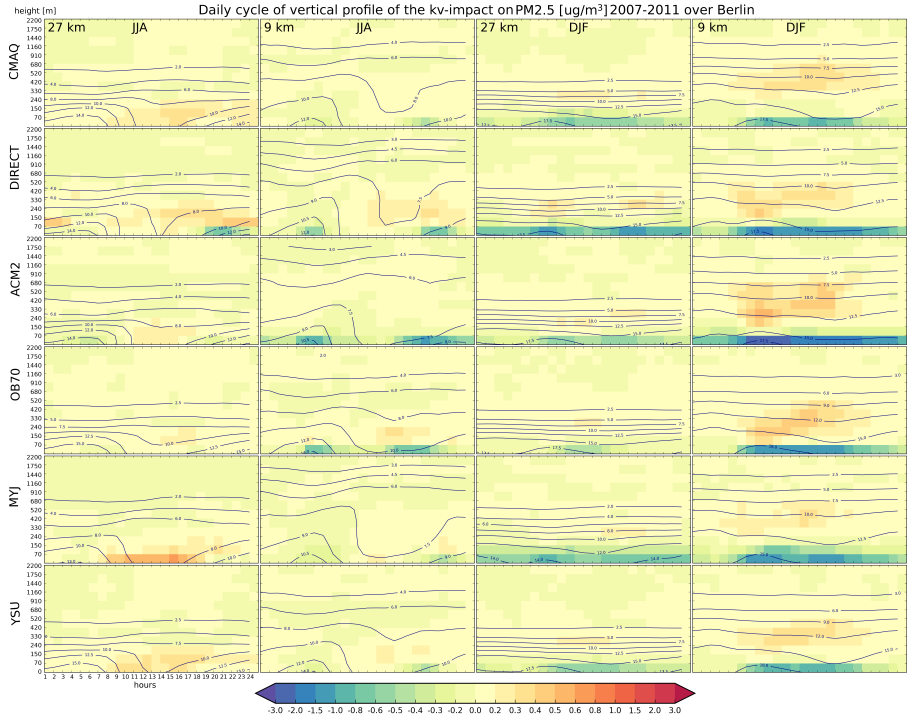


**Figure 24.** The impact of the urbanization induced $Kv$ enhancement (i.e. increase of vertical eddy diffusivity) on the diurnal cycle of the $\mathrm{PM2.5}$ profile over Berlin for JJA (columns 1–2) and DJF (columns 3–4) evaluated over the 27 km (columns 1 and 3) and 9 km (columns 2 and 4) domains. Rows correspond to individual $Kv$-methods. Colors mean the difference, contours stand for the absolute concentrations (from the total-impact). Units in $\mu\mathrm{gm}^{-3}$.

https://doi.org/10.5194/acp-2019-486
Preprint. Discussion started: 26 June 2019


Atmospheric Chemistry and Physics Discussions

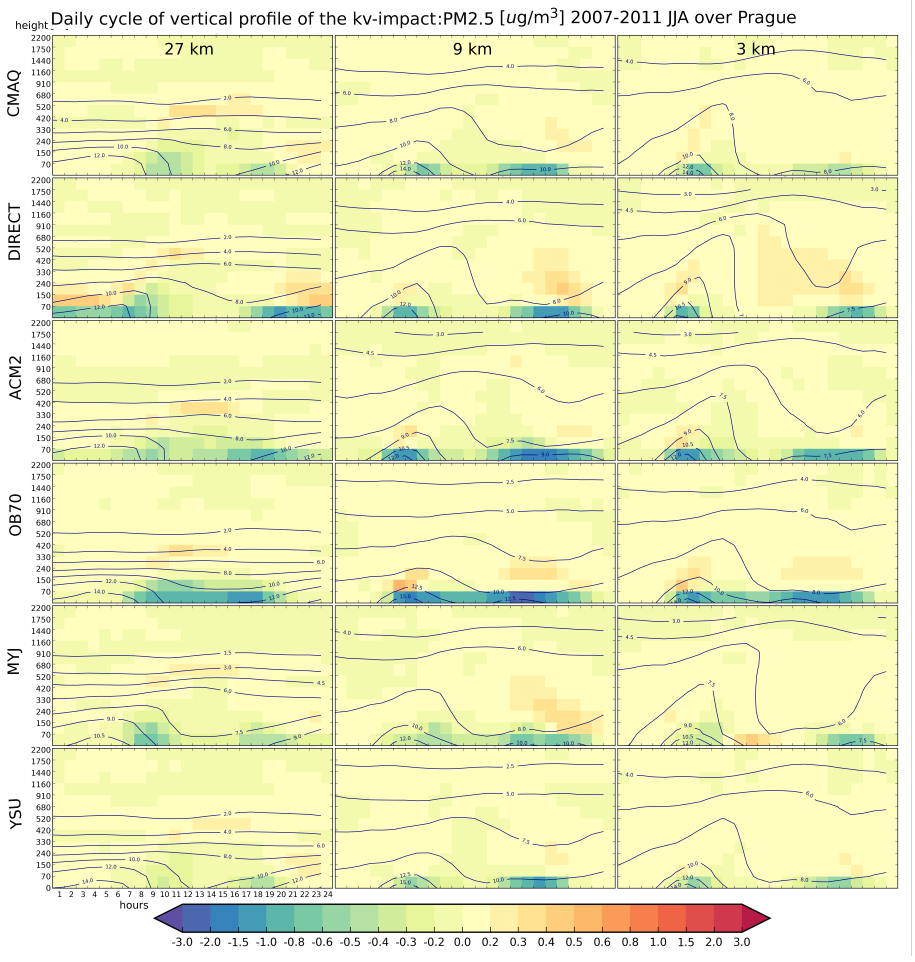


**Figure 25.** The impact of the urbanization induced $Kv$ enhancement (i.e. increase of vertical eddy diffusivity) on the diurnal cycle of the $\mathrm{PM2.5}$ profile over Prague for JJA. Columns represent the three resolutions (27km, 9km and 3 km, from left to right). Rows correspond to individual $Kv$-methods. Colors mean the difference, contours stand for the absolute concentrations (from the total-impact). Units in $\mu\mathrm{gm}^{-3}$.

https://doi.org/10.5194/acp-2019-486
Preprint. Discussion started: 26 June 2019


Atmospheric Chemistry and Physics Discussions

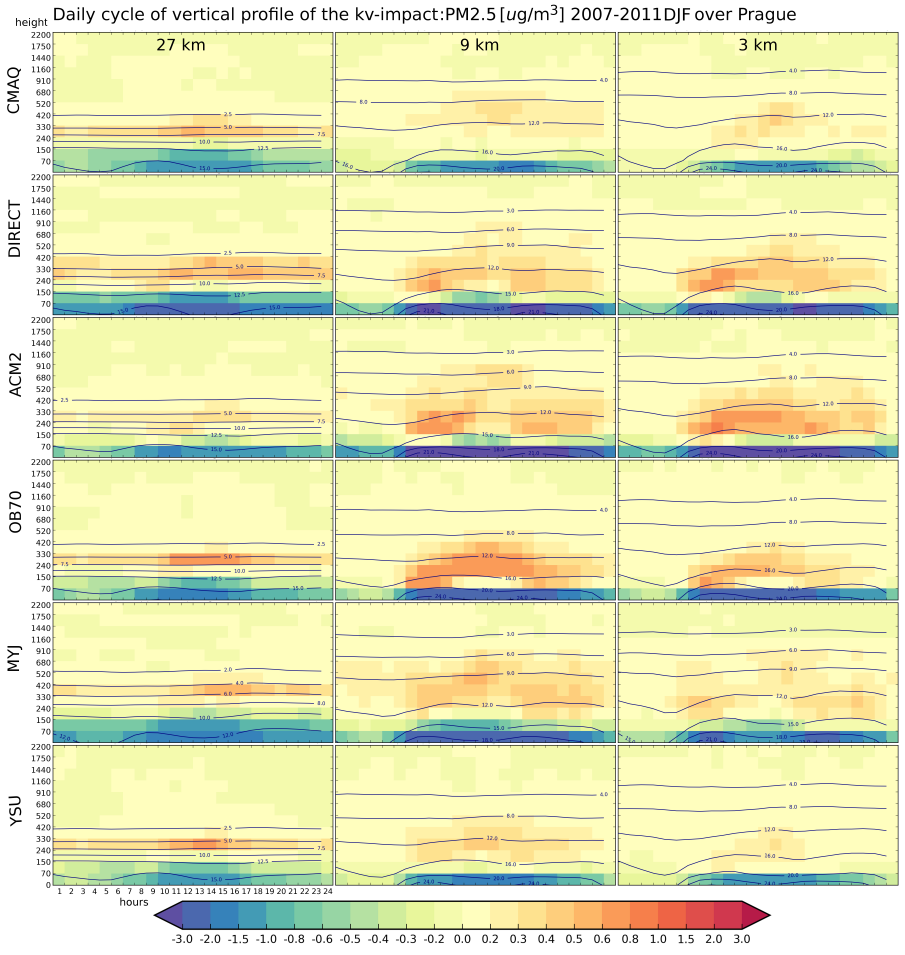


**Figure 26.** Same as Fig. 25 but for DJF.

https://doi.org/10.5194/acp-2019-486
Preprint. Discussion started: 26 June 2019


Atmospheric Chemistry and Physics Discussions

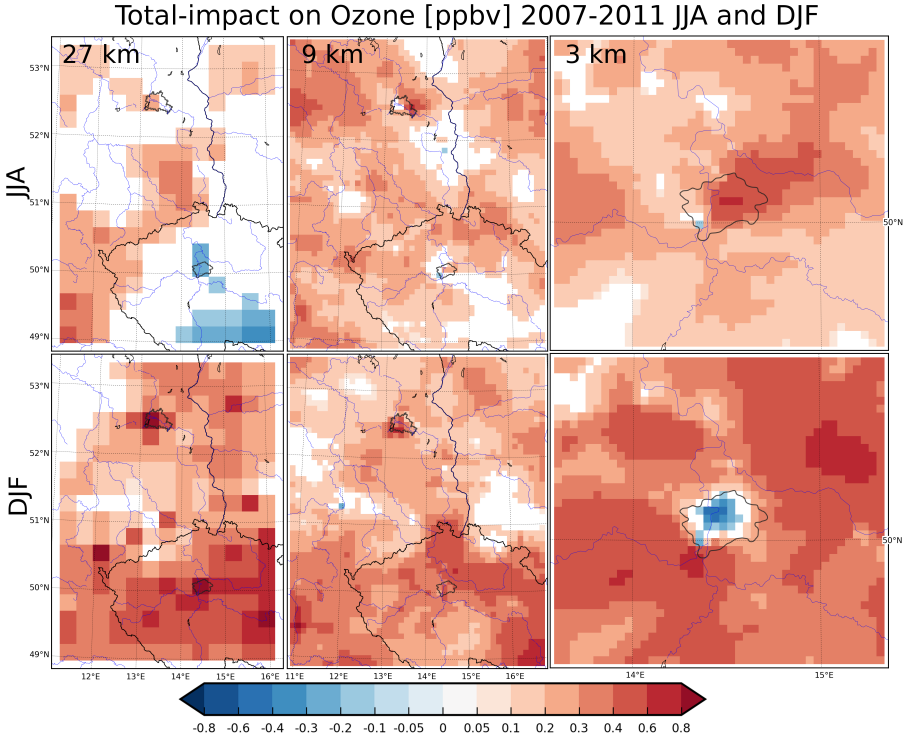


**Figure 27.** The total impact of urban meteorological changes (i.e. temperature, humidity, wind and vertical eddy diffusivity) on surface $O_3$ concentrations in ppbv for the 27, 9 and 3 km resolutions (left to right) for JJA (top) and DJF (bottom). Shaded areas represent statistically significant changes on the 98% threshold level using two tailed t-test. The default CMAQ $Kv$ method was invoked in this calculation. The geographic location of Berlin and Prague is indicated by their administrative boundary.

https://doi.org/10.5194/acp-2019-486
Preprint. Discussion started: 26 June 2019


Atmospheric Chemistry and Physics Discussions

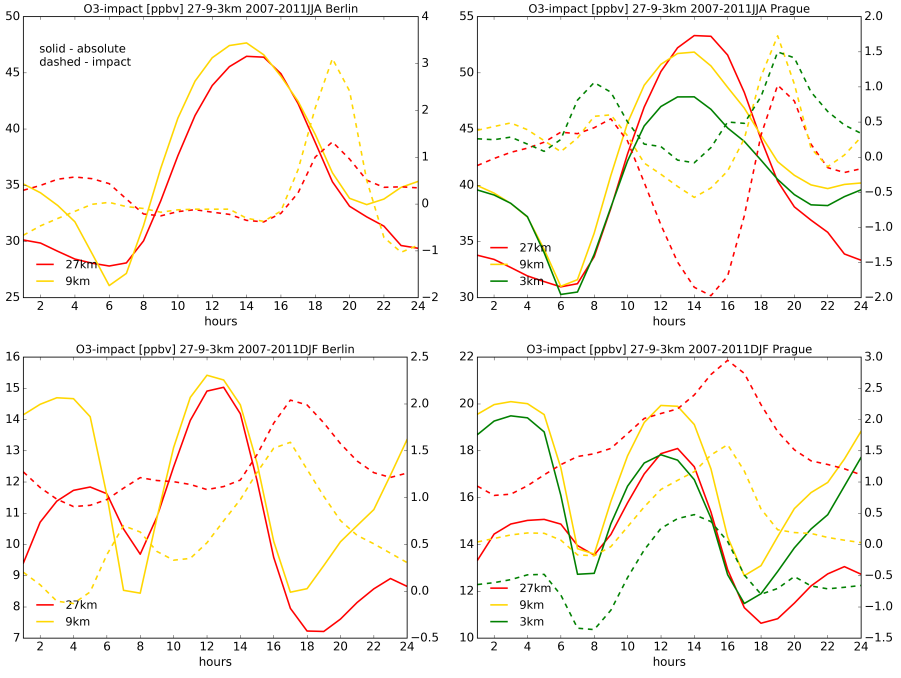


**Figure 28.** The diurnal cycle of the absolute ozone concentrations (solid) as well as the total-impact (i.e. the $t+q+uv+kv$-impact; dashed) above Berlin (left) and Prague (right) for JJA (top) and DJF (bottom) in ppbv. Red, orange and green colors stamd for 27km, 9km and 3 km resolutions, respectively.

https://doi.org/10.5194/acp-2019-486
Preprint. Discussion started: 26 June 2019


Atmospheric Chemistry and Physics Discussions

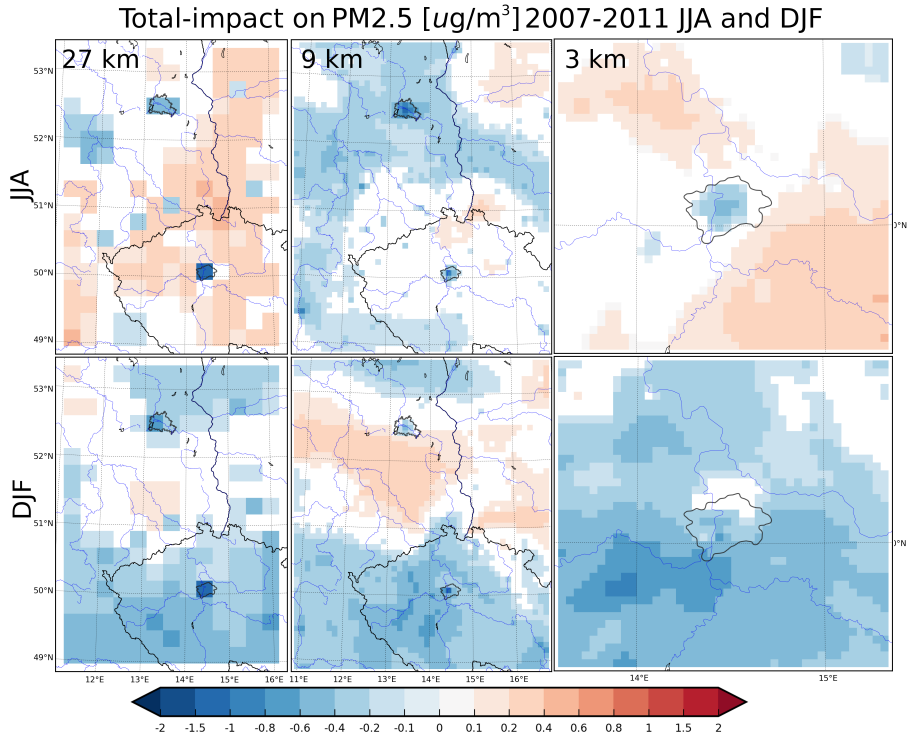


**Figure 29.** The total impact of urban meteorological changes (i.e. temperature, humidity, wind and vertical eddy diffusivity) on surface PM2.5 concentrations in ppbv for the 27, 9 and 3 km resolutions (left to right) for JJA (top) and DJF (bottom). Shaded areas represent statistically significant changes on the 98% threshold level using two tailed t-test. The default CMAQ $Kv$ method was invoked in this calculation. The geographic location of Berlin and Prague is indicated by their administrative boundary.

https://doi.org/10.5194/acp-2019-486
Preprint. Discussion started: 26 June 2019


Atmospheric Chemistry and Physics Discussions

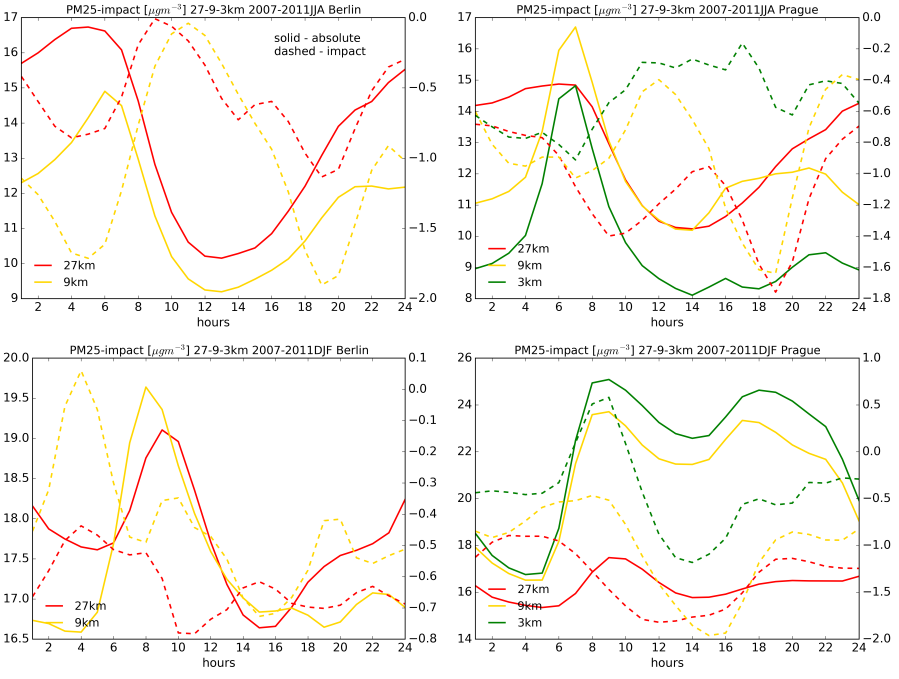


**Figure 30.** The diurnal cycle of the absolute PM2.5 concentrations (solid) as well as the total-impact (i.e. the $t+q+uv+kv$-impact; dashed) above Berlin (left) and Prague (right) for JJA (top) and DJF (bottom) in $\mu gm^{-3}$. Red, orange and green colors stamd for 27km, 9km and 3 km resolutions, respectively.